Acrylic acid and related dimethylated sulfur compounds in the Bohai and Yellow Seas during summer and winter

Xi Wu[2,3], Pei-Feng Li[2,3], Hong-Hai Zhang[1,2,3], Mao-Xu Zhu[1,2,3], Chun-Ying Liu[1,2,3], Gui-Peng Yang[1,2,3]

[1]Key Laboratory of Marine Chemistry Theory and Technology, Ministry of Education, Qingdao, 266100, China
[2]Laboratory for Marine Ecology and Environmental Science, Qingdao National Laboratory for Marine Science and Technology, Qingdao, 266071, China
[3]College of Chemistry and Chemical Engineering, Ocean University of China, Qingdao, 266100, China

Correspondence to: Mao-Xu Zhu (zhumaoxu@ouc.edu.cn); Chun-Ying Liu (roseliu@ouc.edu.cn)

Abstract. Spatio-temporal distributions of dissolved acrylic acid (AAd) and related biogenic sulfur compounds including dimethylsulfide (DMS) and dissolved and total dimethylsulfoniopropionate (DMSPd and DMSPt) were investigated in the Bohai Sea (BS) and Yellow Sea (YS) during summer and winter. AAd and DMS production from DMSPd degradation and AAd degradation were studied. Significant seasonal variations of AAd and DMS(P) were observed. AAd presented similar distributions during summer and winter, that is, relatively high values of AAd emerged in the BS and the northern YS and concentrations decreased from inshore to offshore areas in the southern YS. Due to strong biological production from DMSP and abundant terrestrial inputs from rivers in summer, AAd concentrations in surface seawater during summer (30.01 nmol L^{-1}) were significantly higher than those during winter (14.98 nmol L^{-1}). The average concentration sequence AAd > DMSPt > DMS > DMSPd at transects during summer illustrated particulate DMSP (DMSPp) as a DMS producer and terrestrial sources of AAd, whereas the sequence in winter was AAd > DMSPt > DMSPd > DMS. High values of AAd and DMS(P) were mostly observed in the upper layers with occasional high values at bottom. High AAd concentrations in porewater which could be transported into the bottom water might result from the cleavage of intracellular DMSP and reduce bacterial metabolism in sediments. In addition, the degradation/production rates of biogenic sulfur compounds were obviously higher in summer than those in winter and the removal of AAd was mainly attributed to the microbial consumption. Other sources of AAd besides the production from DMSPd was also proved.

1 Introduction

Dimethylsulfide (DMS), biologically derived from the enzymatic cleavage of dimethylsulfoniopropionate (DMSP), is the dominant volatile sulfur compound released from the ocean to the atmosphere (Lovelock et al., 1972; Dacey and Wakeham, 1986). The annual emission of DMS from the ocean contributes 28.1 (17.6–34.4) Tg S to the atmosphere (Lana et al., 2011). Moreover, DMS is correlated with the natural acidity of rain (Nguyen et al., 1992). DMS produced in surface waters can chemically influence the marine system, global sulfur cycle, and global climate. The CLAW hypothesis pointed that the oxidation products of DMS are the major sources of cloud condensation nuclei (CCN), which lead to an increase in aerosol albedo over the ocean and consequently to a decrease in solar radiation on Earth's surface (Charlson et al., 1987; Malin et al., 1992; Zindler et al., 2012), although recent studies argued that other sources, for example, bubble bursting at the ocean surface, are the major contributions to CCN on global scales (Quinn and Bates, 2011). Therefore, more studies are needed to further our understanding of the potential links between DMS and climate changes.

DMSP, the biochemical precursor of DMS (Malin and Erst, 1997; Alcolombri et al., 2015), is produced by marine phytoplankton and marine heterotrophic bacteria (Keller et al., 1989; Curson et al., 2017). As an antioxidant, a cryoprotectant, or an osmolyte in marine phytoplankton, the production of DMSP is influenced by environmental parameters such as salinity (Stefels, 2000), temperature (Kirst et al., 1991), and oxidative stress (Sunda et al., 2002).

DMSP distributions are also controlled by phytoplankton species, among which diatoms, flagellates, prochlorophytes and cyanobacteria are low producers of DMSP (McParland and Levine, 2019). Furthermore, DMSP provides considerable sulfur and carbon sources for microbial food web. In addition, the degradation of DMSP is mainly through two pathways. The major one is demethylation, a complicated process generating different ultimate products through different enzymes possibly including methanethiol, hydrogen sulfide, and acrylic acid (AA) (Taylor and Visscher, 1996; Bentley and Chasteen, 2004; Reisch et al., 2011). The other pathway is enzymatic cleavage of DMSP mostly into equimolar DMS and AA by phytoplankton (Steinke et al., 2002) and bacteria (Ledyard and Dacey, 1996), a minor pathway with its contribution to DMSP degradation only 10%, on average. (Reisch et al., 2011).

As chemically the simplest unsaturated carboxylic acid, AA in coastal seawater is not only derived from DMSP cleavage, but also from anthropogenic contamination via river discharges (Sicre et al., 1994). The removal of AA is mainly through two mechanisms, that is, photochemical (Bajt et al., 1997; Wu et al., 2015) and microbial degradations (Noordkamp et al., 2000). AA plays diverse roles in the marine systems. For example, AA is an important carbon source to the microbial community (Noordkamp et al., 2000), while it also acts as an antibacterial agent (Sieburth, 1960; Slezak et al., 1994). Furthermore, the presence of AA functions as grazing-activated chemical defense and thus inhibits the predation of phytoplankton by microzooplankton (Wolfe et al., 1997).

Many aspects of DMS and DMSP including spatio-temporal distributions, degradation, sea-to-air fluxes, and particle size fractionation have been well documented (Lana et al., 2011; Levine et al., 2012; Yang et al., 2014; Espinosa et al., 2015; Tyssebotn et al., 2017). Up to date, however, the biogeochemistry of AA itself in the oceans and the roles of AA in the marine sulfur cycle and the microbial community has received only limited attention. Tan et al. (2017) and Wu et al. (2017) reported spatial distributions of AA in the Changjiang Estuary and the East China Sea. Liu et al. (2016) investigated the spatial and diurnal variations of AA in the Bohai Sea (BS) and Yellow Sea (YS) during autumn and measured the apparent production rates of AA through DMSP degradation by incubations. However, seasonal variations, source and removal of AA, and the key factors controlling these processes still remain unclear, and thus further studies are needed to better understand the biogeochemical cycle of sulfur in the oceans. In this study, we investigated horizontal and vertical distributions of dissolved AA (AAd) and related dimethylated sulfur compounds in the BS and YS in different seasons (summer and winter) to determine if temperature, phytoplankton and bacteria species and abundance were key controlling factors on AA dynamics. In addition, it was the first time to collect AAd samples in porewater of surface sediment during summer in the BS and YS. We also examined the degradation of dissolved DMSP (DMSPd) and AAd simultaneously through on-deck incubations during summer and winter to understand production and consumption mechanisms of AA, DMS, and DMSP, to explore the influencing factors (i.e. changes of bacteria species and abundance) of microbial degradation, and to indicate other potential sources of AA. This study is expected to provide insightful information on sulfur cycling from the view of AA in the marginal seas.

2 Material and methods

2.1 Study area

The BS, the largest inner sea in China, is surrounded by Tianjin City, Hebei Province, Shandong and Liaodong Peninsulas. The total water area of the sea is 7.7×10^4 km^2 and the average water depth is 18 m. The hydrological conditions of the BS are substantially influenced by discharges from over 40 rivers, including the Yellow River, Haihe, Daliaohe, and Luanhe (Ning et al., 2010). Especially, the Yellow River, the world's second largest river in terms of sediment load, brings large amounts of particulates and nutrients to the BS. The YS, which is separated from the BS by the Bohai Strait, is a shallow semi-enclosed marginal sea located between the Chinese mainland and the Korean Peninsula, with a total

water area of 3.8 $\times 10^5$ km^2 and a mean depth of 44 m. The YS is divided into northern Yellow Sea (NYS) and southern Yellow Sea (SYS) by a line between Chengshan Cape on the Shandong Peninsula and Changshanchuan on the Korean Peninsula. The BS and YS are greatly affected by complicated water currents and two main water masses including the Bohai Sea Coastal Current (BSCC), the Yellow Sea Coastal Current (YSCC), the Korea Coastal Current (KCC), the Yellow Sea Warm Current (YSWC), the Changjiang River Diluted Water (CRDW), and the Yellow Sea cold water mass (YSCWM) (Lee et al., 2000; Su, 1998) (Fig. 1). Moreover, anthropogenic pollution in both China and Korea coasts has notable effects on the ecosystems including species diversity and community structure of phytoplankton and benthos in the BS and YS (Liu et al., 2011).

2.2 Sampling

Two cruises were conducted aboard the R/V ‘‘Dong Fang Hong 2’’ in the BS and YS from August 17th to September 5th 2015 (summer) and from January 14th to February 1st 2016 (winter). The summer cruise covered 52 grid stations and three transects and the winter cruise contained 39 grid stations and two transects (Fig. 1). Seawater samples were collected using 12 L Niskin bottles mounted on a Seabird 911+ Conductivity-Temperature-Depth (CTD) sensor (Sea-Bird Electronics, Inc., USA). Temperature and salinity were measured by the CTD sensor. Water samples were transferred from the Niskin bottles to 250 mL brown glass bottle through silicone tubing. While filling the bottles, the samples were allowed to overflow from the top of the bottle to eliminate any headspace in an effort to minimize partitioning into the gas phase. Sediments were collected using a stainless-steel box-corer and sub-sampled to a depth of ca. 3 cm at 12 stations shown in Table 1 during summer cruise.

2.3 Analytical procedures

DMS concentrations in all samples were immediately measured onboard upon sampling with a purge-and-trap technique modified from Andreae and Barnard (1983) and Kiene and Service (1991). A 2 mL aliquot of seawater sample extracted from the 250 mL brown glass bottle using a 2 mL glass syringe and filtered by syringe filtration through 25 mm Whatman glass fiber (GF/F) filter (Li et al., 2016) was directly injected into a glass bubbling chamber and extracted with high purity nitrogen at a flow rate of 40 mL min^{-1} for 3 min. Then, the sulfur gases were dried through Nafion gas sample dryer (Perma Pure, USA) and trapped in a loop of Teflon tubing immersed in liquid nitrogen (-196 °C). After extraction, the Teflon tubing was heated in boiling water and desorbed gases were introduced into a 14B gas chromatograph (Shimadzu, Japan) equipped with a flame photometric detector and a 3 m × 3 mm glass chromatographic column packed with 10% DEGS on Chromosorb W-AW-DMCS. The analytical precision of DMS was generally better than 10% and the detection limit was 0.4 nmol L^{-1} (Yang et al., 2015a).

A 4 mL aliquot of seawater was filtered under gravity through 47 mm Whatman GF/F filter (Kiene and Slezak, 2006) for DMSPd analysis. A 10 mL aliquot of seawater without filtering was used for total DMSP (DMSPt) analysis. In order for steady DMSP concentration and oxidation of endogenous DMS, 100 µL and 40 µL of 50 wt% sulfuric acid were added into samples for DMSPt and DMSPd analysis, respectively (Shooter and Brimblecombe, 1989). To fully oxidize pre-existing gaseous DMS, the DMSPt and DMSPd samples were incubated in the dark at room temperature for 2 days. Before analysis, the samples were injected with 300 µL of 10 mol L^{-1} KOH solutions and stored in the dark at 4 °C for at least 24 h to allow a complete conversion of DMSP into DMS. DMS concentration measured was used to estimate DMSP concentration according to 1:1 stoichiometry (Dacey and Blough, 1987). This method gave the same precision and detection limit for DMSP as DMS. DMS and DMSP data in surface seawater has published in Master theses (Jin, 2016; Sun, 2017).

Seawater samples for AAd analyses were collected directly from the Niskin bottles and filtered under gravity through a pre-cleaned 0.2 μm AS 75 Polycap filter capsule (a nylon membrane with a glass microfiber pre-filter enclosed in a polypropylene housing; Whatman Corporation, USA) (Wu et al., 2015). The filtrate was transferred to a 40 mL glass vial with a Teflon™-lined cap and stored at 4 °C. Porewater samples for AAd analyses were extracted from surface sediments via Rhizon soil moisture samplers (0.1 μm porous polymer, Rhizosphere Research, Wageningen, the Netherlands) according to Seeberg-Elverfeldt et al. (2005). All porewaters were stored at 4 °C and filtered through 0.22 μm polyethersulfone syringe filters (Membrana Corporation, Germany) before analysis. AAd seawater and porewater samples were analyzed using a high performance liquid chromatograph (L-2000, Hitachi Ltd., Japan) according to Gibson et al. (1996). An Agilent SB-Aq-C18 column and the eluent of 0.35% H_3PO_4 (pH = 2.0) at a flow rate of 0.5 mL min^{-1} were used to separate AAd. The column eluate was detected by a UV detector at 210 nm. Analytical precision was between 1.3% and 1.6% and the detection limit was 4 nmol L^{-1} (Liu et al., 2013).

For Chlorophyll *a* (Chl *a*) analysis, 300 mL of seawater were filtered through Whatman GF/F filters. Then the filtrates were soaked in 10 mL of 90% acetone and kept in the dark at 4 °C. Contents of Chl *a* were measured using an F-4500 fluorescence spectrophotometer (Hitachi, Japan) according to Parsons et al. (1984) after 24 h. In addition, the concentrations of nutrients (including PO_4^{3-}, NO_3^-, NO_2^-, NH_4^+, and SiO_3^{2-}) were analyzed using a nutrient automatic analyzer (Auto Analyzer 3, SEAL Analytical, USA). Phytoplankton data recorded by Utermöhl method and bacteria data measured by qPCR were collected from Zhang (2018) and Liang et al. (2019), respectively. Analytical samples for DMS, DMSPd, DMSPt, AAd, Chl *a*, and nutrients were run in duplicate.

2.4 Incubation experiments

The incubation experiments for DMSPd and AAd degradation were conducted on deck using seawater collected at stations H19, H26, B12, B17, B53, and B63 in summer and at H19, H26, B12, and B16 in winter according to Wu et al. (2017). To determine degradation rates of DMSPd and production rates of DMS and AAd, unfiltered seawater samples were incubated in two 250 mL gas-tight glass syringes (wrapped in aluminum foil) in the dark at in situ temperature. Before the incubations, 80 μL of concentrated DMSPd solution (0.2 mmol L^{-1}) were added into the two syringes to reach an initial concentration of DMSPd higher than 50 nmol L^{-1}. One syringe was used as treatment group, the other was used as control by injecting with glycine betaine (GBT, final concentration of 50 μmol L^{-1}, 1000× the concentration of added DMSPd) to inhibit microbial degradation of DMSP within a short time (Kiene and Service, 1993; Kiene and Gerard, 1995) because it is chemically and physiologically similar to DMSP and acts as a competitive inhibitor of DMSP (Kiene et al., 1998). After 0, 3, and 6 h, 25 mL aliquots of samples were taken from the incubations for measurements of DMSPd, DMS, and AAd concentrations. Linear regression equations were fit to the DMSPd, DMS, and AAd time course data and the apparent rates were estimated as the differences between the slopes of samples with and without GBT.

Two pathways of AAd degradation, that is, photochemical consumption and microbial consumption, were experimentally investigated in this study. For photochemical consumption of AAd, a drop of oversaturated NaN_3 solution was added into 300 mL seawater samples (the final concentration was approximately 1 mmol L^{-1}) to eliminate microbial consumption of AAd. After filtration, the seawater samples were immediately injected into a 125 mL photic quartz tube and a 125 mL photophobic quartz tube (as a control) to initiate photochemical degradation. 10 mL aliquots of samples were taken for analyses of AAd at 0, 3, and 6 h. Linear regression equations were fit to the AAd time course data and the photochemical degradation rates of AAd were calculated based on the differences between the slopes of samples in the photic and photophobic quartz tubes (Wu et al., 2015).

For microbial consumption of AAd, unfiltered seawater samples were used for incubations in 100 mL glass syringes (wrapped in aluminum foil) in the dark at in situ temperature. Prior to incubation, concentrated AAd was added into one

syringe to reach an initial concentration 10-50 times as high as the background concentration. Another seawater sample without exogenous AAd addition was used as a control. 10 mL aliquots of samples were taken for determination of AAd at 0, 3, and 6 h. Linear regression equations were fit to the AAd time course data and the microbial degradation rates of AAd were estimated as the differences between the slopes of samples with exogenous AAd addition and the control (Wu et al., 2015). Duplicate samples were analyzed for AAd, DMS, and DMSPd in all the incubation experiments.

3 Results

3.1 Horizontal distributions of AAd in the BS and YS

In summer, Chl *a* contents in surface seawater were in the range of 0.01-8.91 μg L^{-1}, with an average value of 1.95 ± 2.31 μg L^{-1}. The contents in the BS were relatively high and an extremely high value (7.07 μg L^{-1}) occurred in the center of the sea, while those concentrations decreased gradually from inshore to offshore areas in the NYS and the northern area of the SYS. The minimum value of Chl *a* emerged in the center of the SYS, while the maximum appeared in the southern area of the SYS (station H37).

AAd concentrations in surface seawater during summer ranged from 10.53 to 92.29 nmol L^{-1}, with a mean of 30.01 ± 21.12 nmol L^{-1}, and the concentrations generally decreased from the north to the south (Fig. 2 and Table 1). The average values in the BS and the NYS were 40.76 ± 24.80 and 38.89 ± 22.61 nmol L^{-1}, respectively, higher than the average value of the whole study area, while the mean value in the SYS was 18.02 ± 7.70 nmol L^{-1}, just more than half of the average value of the whole study area, even though the Chl *a* values were relatively high in the SYS. In addition, AAd was positively dependent on temperature in the NYS (Table 2). DMS and DMSP presented by Jin (2016) showed diminishing tendency from inshore to offshore areas (Fig. 3), which was coupled to the distribution pattern of Chl *a*. DMS and DMSP also presented higher values in the BS than in the YS, similar to the case of AAd.

In winter, Chl *a* contents in surface seawater ranged from 0.16 to 0.99 μg L^{-1} (mean: 0.47 ± 0.21 μg L^{-1}) and decreased from inshore to offshore areas in general. AAd concentrations varied from 4.28 to 42.05 nmol L^{-1} (mean: 14.98 ± 7.72 nmol L^{-1}), and high concentrations appeared near the Chengshan Cape where high values of Chl *a*, DMS, DMSP, phytoplankton abundance were also observed (Figs. 2 and 3) (Sun, 2017; Zhang, 2018). Chl *a*, AAd, DMS, and DMSPd all showed declining tendency from inshore to offshore areas in the SYS. Note that the AAd concentrations in the BS (15.94 ± 10.49 nmol L^{-1}), the NYS (14.53 ± 7.64 nmol L^{-1}), and the SYS (14.91 ± 6.31 nmol L^{-1}) had no significant differences.

3.2 Vertical distributions of AAd, DMS, and DMSP in the BS and YS

In summer, three transects of B57-63, B12-17, and H19-26, which were located in the BS, the NYS, and the SYS, respectively, were chosen to study the vertical distributions of AAd, DMS, and DMSP. Along transect B57-63, the Chl *a*, AAd, DMS, DMSPd, and DMSPt concentrations were within the ranges of 0.15-7.07 μg L^{-1} (mean 1.58 ± 1.88 μg L^{-1}), 11.08-73.06 nmol L^{-1} (mean 36.36 ± 23.57 nmol L^{-1}), 2.57-8.79 nmol L^{-1} (mean 5.51 ± 2.01 nmol L^{-1}), 0.72-3.37 nmol L^{-1} (mean 1.56 ± 0.84 nmol L^{-1}), and 4.12-56.61 nmol L^{-1} (mean 22.94 ± 21.28 nmol L^{-1}), respectively. All of the compounds presented high values in the upper layers. Meanwhile, Chl *a* and AAd presented relatively high values at the bottom of station B61 and B57, respectively (Fig. 4).

Along transect B12-17, the Chl *a* and DMS concentrations varied from 0.18 to 2.87 μg L^{-1} and from 0.74 to 15.76 nmol L^{-1}, with means of 0.92 ± 0.96 μg L^{-1} and 7.37 ± 4.50 nmol L^{-1}, respectively. Low values of Chl *a* occurred in the bottom seawater of the transect and in the water column of station B15, while Chl *a* and DMS presented maximum values at the 15 m depth of stations B13 and 25 m depth of station B15, respectively (Fig. 4). Concentrations of DMSPd, DMSPt, and

AAd were in the ranges of 0.36-2.01 nmol L^{-1}, 1.90-63.03 nmol L^{-1}, and 12.77-102.988 nmol L^{-1}, with averages of 1.12 ± 0.48 nmol L^{-1}, 15.45 ± 17.98 nmol L^{-1}, and 34.60 ± 26.00 nmol L^{-1}, respectively. Those concentrations declined generally with depth and highest concentrations were observed in the surface layers of station B12 and B13. Yang et al. (2015a) also found maximum values of DMS and DMSP in the upper water column along transect B12-17 during late fall, which were restricted mostly to the euphotic layer. High values of AAd also occurred in the bottom water of stations B13 and B17. DMSPd and DMSPt showed a strong positive correlation (Table 2), while AAd did not have a correlation with DMSP. Meanwhile, the average value of AAd was more than 2 times of that of DMSPt, the precursor of AAd, which demonstrated that terrestrial inputs were an important contribution to AAd along transect B12-17.

Transect H19-26 was affected by the YSCWM in summer, as indicated by low temperature (<10 °C) below 40 m water depth. A tidal front divided the transect into a well-mixed shallow water area (station H19) and a stratified deep-water area occupied by the YSCWM (stations H21-H26) (Fig. 4). Concentrations of Chl *a*, DMS, DMSPd, DMSPt, and AAd were in the ranges of 0.12-1.50 μg L^{-1} (mean 0.58 ± 0.39 μg L^{-1}), 0.79-21.98 nmol L^{-1} (mean 6.44 ± 5.14 nmol L^{-1}), 0.61-21.59 nmol L^{-1} (mean 3.05 ± 4.92 nmol L^{-1}), 1.11-55.14 nmol L^{-1} (mean 13.67 ± 12.90 nmol L^{-1}), and 13.19-85.86 nmol L^{-1} (mean 22.24 ± 18.25 nmol L^{-1}), respectively. DMSPd, DMSPt, and AAd showed stratified distributions similar to temperature, but Chl *a* and DMS did not display obviously stratified distributions. The Chl *a* contents generally decreased from inshore to offshore areas with minimum values in the medium and bottom layers of offshore stations. High values of the sulfur compounds in the surface seawater and higher concentrations in the YSCWM region than those in the well mixed shallow water region were in line with the results of Yang et al. (2015b). In addition, there was a relatively high value of DMS in the bottom layer of station H23. There were no significant correlations among AAd, DMS, DMSPd, and DMSPt, though these compounds showed similar patterns of spatial distribution. DMSPt showed a positive correlation with temperature and a negative correlation with salinity (Table 2). Many other investigations also reported the analogous correlations (Shenoy and Patil, 2003; Deschaseaux et al., 2014; Wu et al., 2017).

In winter, transect B57-63 was inaccessible for sampling due to frozen condition, thus we only reported the results of transect B12-16 in the NYS and transect H19-26 in the SYS. Along transect B12-16, the Chl *a*, DMS, DMSPd, DMSPt, and AAd concentrations were in the ranges of 0.17-1.56 μg L^{-1}, 1.12-4.56 nmol L^{-1}, 1.54-4.55 nmol L^{-1}, 5.33-24.50 nmol L^{-1}, and 13.94-27.69 nmol L^{-1}, with averages of 0.53 ± 0.43 μg L^{-1}, 1.99 ± 1.02 nmol L^{-1}, 2.92 ± 0.82 nmol L^{-1}, 11.44 ± 5.89 nmol L^{-1}, and 17.68 ± 5.21 nmol L^{-1}, respectively. Furthermore, Chl *a*, DMS, and DMSPt presented homogeneous distributions from the surface to the bottom, while DMSPd and AAd were heterogeneously distributed with minimum values appearing at the surface and maximum values at the bottom (Fig. 5).

Along transect H19-26, The concentrations of Chl *a* and DMSPt varied from 0.13 to 0.42 μg L^{-1} and from 6.12 to 19.92 nmol L^{-1} with means of 0.28 ± 0.09 μg L^{-1} and 11.88 ± 3.97 nmol L^{-1}, respectively. They declined from inshore to offshore areas, while DMS (0.52-1.35 nmol L^{-1}, average 0.96 ± 0.29 nmol L^{-1}) and DMSPd (1.92-6.06 nmol L^{-1}, average 3.06 ± 1.07 nmol L^{-1}) showed decreasing trends from the surface to the bottom (Fig. 5). AAd concentrations ranged from 11.04 to 39.47 nmol L^{-1} (mean 17.08 ± 6.72 nmol L^{-1}) and did not present significant variations along transect H19-26 except the maximum value at the bottom of station H24.

AAd concentrations in porewater of surface sediments during summer were 13.52-136.42 μmol L^{-1}, with an average of 73.03 ± 46.05 μmol L^{-1} (Table 3), but no significant correlation of AAd concentrations between porewater and bottom seawater was observed. The maximum value of AAd was observed at station H23, meanwhile, the AAd concentrations were all relatively high in sediment porewater of transect H19-26 in the SYS, with an average of 121.79 μmol L^{-1}. Stations at transect H10-18 in the SYS and transect B12-17 in the NYS presented similar AAd concentrations (about 45 μmol L^{-1}), while stations (B61 and B63) at the BS showed big differences. Generally, AAd concentrations in porewater of surface sediments in the YS were higher than those in the BS.

3.3 Degradation of DMSPd and AAd in the BS and YS

The DMSPd and AAd degradation experiments were conducted using seawater at the endpoint stations of investigated transects in the BS and YS during the two cruises. Production and/or degradation rates of DMSPd, DMS, and AAd were summarized in Table 4. In summer, the rates of DMS production at all stations were significantly lower than the rates of DMSPd degradation (Mann-Whitney test, $p = 0.01$), while rates of AAd production at stations B12 and B63 were a little higher than the rates of DMSPd degradation. The rates of AAd production at all stations were higher than those of DMS production (Mann-Whitney test, $p < 0.05$). Enzymatic cleavage ratio of DMSP can be estimated using DMS production rate/DMSPd degradation rate. The ratios were within the range of 7.8%-64.5%, with a mean of 27.7%. The maximum rates of DMSPd degradation (5.76 ± 0.47 nmol L^{-1} h^{-1}) and DMS (2.71 ± 0.36 nmol L^{-1} h^{-1}) and AAd (5.20 ± 0.40 nmol L^{-1} h^{-1}) production appeared at stations B57 and B63 in the BS, respectively. The minimum rates of DMS (0.29 ± 0.12 nmol L^{-1} h^{-1}) and AAd (1.15 ± 0.31 nmol L^{-1} h^{-1}) production occurred at stations H26 and H19 in the SYS, respectively. Though the rates of AAd microbial degradation at all stations were extremely high compared to the rates of AAd production and AAd photochemical degradation due to the addition of exogenous AAd at the beginning of incubation, the comparison of AAd microbial degradation rates between different stations were still rational. Specifically, AAd microbial degradation rates at inshore stations were higher than those at offshore stations and the rates in the NYS were comparatively lower than those in the BS and the SYS. Moreover, the average AAd photochemical degradation rates in the SYS were higher than those in the BS and the NYS. Assuming that DMSPd and AAd degradation follow first-order kinetics, turnover times of DMSPd and rate constants of AAd microbial and photochemical degradation were calculated (Table 4).Turnover times of DMSPd in the BS and YS basically fell in the range of 0.03-2.8 d which were estimated in earlier studies using radioisotopes, inhibitors and low-level additions methods in worldwide oceanic regions (Ledyard and Dacey, 1996; Kiene and Linn, 2000a; Simó et al., 2000). In addition, the AAd microbial degradation rate constants at most stations were higher than the AAd photochemical degradation rate constants.

In winter, almost all degradation/production rates lowered compared to those in summer. Furthermore, the turnover times of DMSPd in winter were much longer than those in summer (Mann-Whitney test, $p < 0.05$) but still fell in the range of earlier studies. The rates of DMS production were lower than the rates of DMSPd degradation and AAd production (Mann-Whitney test, $p < 0.05$) in winter, which were in accordance with those in summer. Even though the difference of DMS production rates was not large among these stations, the maximum rates of DMSPd degradation (2.26 ± 0.75 nmol L^{-1} h^{-1}), DMS production (0.10 ± 0.02 nmol L^{-1} h^{-1}), and AAd production (1.48 ± 0.29 nmol L^{-1} h^{-1}) were all observed in the SYS, which were different from the case in summer. Enzymatic cleavage ratio of DMSP (3.5%-11.1%; average: 7.0%) in winter were much lower than in summer. The microbial degradation rates of AAd significantly decreased from summer to winter but the rate constants in winter did not show dramatic decline compared to those in summer and even slightly increased at some stations. The AAd microbial degradation rates and rate constants were higher than the photochemical rates and rate constants at most of the stations in winter, which were in accordance with those in summer.

4 Discussion

4.1 Biogeochemical processes influencing on AAd in the surface water of the BS and YS

In summer, the average concentrations of PO_4^{3-} in the BS (0.04 μmol L^{-1}), the NYS (0.05 μmol L^{-1}) and the SYS (0.04 μmol L^{-1}) were similar, however, the average NO_3^-, NO_2^-, and SiO_3^{2-} concentrations in the BS (NO_3^-: 0.89 μmol L^{-1}; NO_2^-: 0.18 μmol L^{-1}; SiO_3^{2-}: 7.91 μmol L^{-1}) were much higher than those in the NYS (NO_3^-: 0.22 μmol L^{-1}; NO_2^-: 0.04 μmol L^-

280 ^{1}; SiO_3^{2-}: 3.26 μmol L^{-1}) and the SYS (NO_3^-: 0.52 μmol L^{-1}; NO_2^-: 0.10 μmol L^{-1}; SiO_3^{2-}: 4.17 μmol L^{-1}). Therefore, the high total nutrients contents due to poor water circulations in the BS promoted phytoplankton productivity and consequently resulted in high Chl *a* contents in the BS (Wei et al., 2004; Wang et al., 2009). Meanwhile, the minimum value of Chl *a* emerged in the center of the SYS could be ascribed to limitation of phytoplankton growth due to low nutrient contents (concentration of total inorganic nutrients < 3 μmol L^{-1}), while the maximum appeared in the southern
285 area of the SYS was due to high concentration of nutrients (total inorganic nutrients concentration of about 15 μmol L^{-1}) delivered via the CRDW (Wei et al., 2010).

AAd concentrations in the BS and YS during summer were an order of magnitude higher than those (0.8-2.1 nmol L^{-1}, median 1.5 nmol L^{-1}) in the northern Gulf of Mexico in September 2011 (Tyssebotn et al., 2017). The reasons for these differences might be related to differences in sample storage, analytical methods and study areas. We stored samples at
290 4 °C, while Tyssebotn et al. (2017) stored at -20 °C. In addition, our study area was highly affected by anthropogenic activities. Relatively higher AAd concentrations in the BS and the NYS than in the SYS during summer implied that terrestrial inputs might play an important role in controlling AAd distribution in the BS and the NYS. It has been reported that Yalu River flows into the NYS with large amounts of organic pollutants including AA (Liu, 2001), and highly populated Chengshan Cape may also be an anthropogenic source of AAd to the NYS. Furthermore, poor water circulation
295 in the semi-enclosed NYS and inner BS favours local accumulations of AAd. On the contrary, SYS is a relatively open water area and thus is much less affected by terrestrial discharges. Moreover, AAd from DMSP degradation was not abundant in the SYS though the Chl *a* values were relatively high, which might be related to the dominance of primary phytoplankton species with low ability of AAd production. Specifically, diatoms, a type of algal with low ability of DMSP and AAd production, dominated in the SYS during summer (Liu et al., 2015). According to Zhang (2018), the maximum
300 phytoplankton abundance in the SYS was 172.39 cell mL^{-1}, among which diatom abundance occupied 146.81 cell mL^{-1}. Furthermore, the diatom/dinoflagellates ratio was 28.96. In addition, some freshwater algae which do not produce DMSP and AAd have been found to distribute in the adjacent area of the Changjiang Estuary (Luan et al., 2006) and the north branch of the Changjiang Estuary flows into the SYS. All of those factors may have led to low AAd concentrations in the SYS.

305 The Chl *a* contents were substantially lower in winter (< 1 μg L^{-1} overall) than those in summer due to lower temperature, light intensity, and phytoplankton activities, while the distribution patterns of Chl *a* in the two seasons were similar, which could be proved by Zhang's (2018) results of phytoplankton abundance. Zhang (2018) found that the average phytoplankton abundance in winter (3.84 cell mL^{-1}) was much lower than that in summer (29.81 cell mL^{-1}), but diatoms (3.83 cell mL^{-1}) were still the dominant type of phytoplankton in winter. Moreover, Sun et al. (2001) also found that
310 diatoms in the study area were mainly made up of small diatoms in winter and larger diatoms in summer.

AAd, DMS, and DMSP concentrations in surface seawater during winter were about 2-4 times lower than those during summer (Table 1) but presented similar distribution patterns. Moreover, Jin (2016) and Sun (2017) found significant positive correlations between DMS(P) and Chl *a* during summer (DMS: $r = 0.418$, $n = 50$, $p < 0.01$; DMSPd: $r = 0.351$, $n = 50$, $p < 0.05$) and winter (DMS: $r = 0.629$, $p < 0.01$; DMSPp: $r = 0.527$, $p < 0.01$), respectively. These phenomena
315 demonstrated that DMS(P) were mainly from biological production and the biological production was stronger in summer than in winter. However, AAd showed no correlations with Chl *a*, nutrients, DMS, and DMSP in the whole study area during summer and winter, which were likely impacted by measuring only dissolved AA. The majority of AA produced from DMSPd degradation would be expected to be stored intracellularly (Kinsey et al., 2016; Tyssebotn et al., 2017), whereas the majority of DMS produced would be expected to be found in the dissolved phase (Spiese et al., 2016).
320 Therefore, AAd was not correlated with other biological parameters but DMS presented good correlations. In addition, terrestrial inputs might affect AAd distributions apart from biological production. Therefore, AAd presented high values

near the Chengshan Cape with intense human activities, where was also the high value area of Chl *a*, DMS, DMSP, and phytoplankton abundance. Nonetheless, terrestrial inputs were weaker in winter than in summer, which resulted in the slightly higher AAd concentrations in the BS than in the YS. AAd, DMS, and DMSP both presented relatively high values in the BS and the NYS and reduced concentrations from inshore to offshore areas in the SYS during summer and winter, which were also consistent with the distribution patterns in the BS and YS during autumn (Liu et al., 2016).

Positive correlation between AAd and temperature in the NYS during summer and in the BS during winter (Table 2) indicated that high temperature might enhance both the biological production and the terrestrial sources of AAd, and positive correlation between AAd and DMSPd in the SYS during summer suggested that AAd in the SYS was mainly produced by DMSPd degradation rather than the terrestrial inputs.

4.2 Biogeochemical processes influencing on AAd, DMS, and DMSP in the vertical profiles of the BS and YS

Along the three transects, high values of AAd, DMS, and DMSP emerged in the bottom water occasionally during summer and winter, which might result from the release from porewater (Andreae, 1985) (Figs. 4 and 5). DMSP showed positive correlations with temperature and negative correlations with salinity along the three transects during summer, while DMS and DMSP presented negative correlations with temperature and salinity during winter, which might be due to a co-correlation of these abiotic parameters themselves. DMS and DMSP had negative correlations with nutrients along the three transects during summer and winter except positive correlations between DMS and nutrients (PO_4^{3-} and SiO_3^{2-}) along transect H19-26 during winter. In addition, positive correlations among DMS, DMSPd, and DMSPt along transect B57-63 and B12-17 during summer and positive correlation between DMSPt and Chl *a* along transect B12-16 during winter indicated DMSP as the phytoplankton-derived precursor of DMS (Table 2).

In summer, the average concentration order was AAd > DMSPt > DMS > DMSPd along the three transects, which was consistent with the order in surface seawater (Table 1). The higher values of DMS than DMSPd might be produced through the intra-cellular cleavage of phytoplankton DMSPp catalyzed by the enzyme DMSP lyase and the photochemical and biological reduction of dimethylsulfoxide (DMSO) to DMS (Asher et al., 2017), while the higher values of AAd than DMSPt indicated that there were terrestrial sources of AAd besides the contribution from in situ DMSP degradation along the three transects. Though there were only small differences in the average concentrations of sulfur compounds among the three transects, the average concentrations of AAd showed significant differences (Kruskal-Wallis test, $p < 0.05$). For instance, AAd concentrations along transect B12-17 (NYS) and transect B57-63 (BS) were higher than those along transect H19-26 (SYS), which was in accordance with those distributions in surface seawater. The high concentration could be ascribed to anthropogenic addition. Average contents of both Chl *a* and DMSPt along the three transects followed the order: B57-63 > B12-17 > H19-26. This suggested that large amounts of phytoplankton biomass might induce high concentrations of DMSPt.

In winter, the average Chl *a* and DMS concentrations along transect B12-16 were about twice as high as those along transect H19-26, which suggested that Chl *a* had a direct controlling effect on DMS production. However, the average concentrations of DMSPd, DMSPt, and AAd along transect H19-26 were quite similar to those along transect B12-16, which implied that the enzymatic cleavage of DMSP enhanced and river discharges did not dominate the concentrations of AAd in winter. The concentration order along both transect H19-26 and transect B12-16 was AAd > DMSPt > DMSPd > DMS. AAd concentrations were only slightly higher than DMSPt, while the DMSPd concentrations exceeded DMS in winter.

A comparison of vertical profiles in different seasons (Figs. 4 and 5, Table 1) indicated that the DMS concentrations declined dramatically (by more than 5 nmol L^{-1}) from summer to winter, and the DMSPd concentrations also displayed significant seasonal variations. The DMSPt concentrations were also a little higher in summer than in winter, consistent

with the seasonal pattern of Chl *a*, which highlighted the control of phytoplankton in DMS(P) production in both the two seasons. The higher AAd concentrations in summer than in winter were a combined result of high phytoplankton biomass and terrestrial inputs in summer. On the whole, the reduced AAd concentrations from summer to winter along transect H19-26 were lower than those along transect B12-17(16), which suggested that terrestrial discharges are an important contribution of AAd concentrations in the NYS, and thus have greatly influenced the spatial distribution.

The AAd concentrations in porewater in our study were much higher than those (50-60 nmol L^{-1}) in Gulf of Mexico reported by Vairavamurthy et al. (1986). The differences might be owing to the differences in sampling, analytical methods and locations. In their study, sediment porewater was obtained by centrifugation of thawed samples that had been kept deep-frozen and they measured only two samples using electron capture gas chromatography, whereas we collected porewater via Rhizon soil moisture samplers connecting to vacuum tubes and analysed samples using a high performance liquid chromatograph. The pressure in vacuum tube might cause cell break in sediments and thus release more AAd in porewater. Moreover, the bacteria abundance and species in the sediments of the BS and YS in 2015 might be different from those in Gulf of Mexico in 1986. Wang (2015) reported δ- and γ-proteobacteria were the dominant taxa in the sediments of the BS and YS, proportion ranging between 24%-70%. Meanwhile, DddY, which is the only known periplasmic DMSP lyase (Li et al., 2017), is widely present in δ- and γ-proteobacteria and can cleave the large amounts of intracellular DMSP (mmol L^{-1} levels) concentrated by DMSP catabolizing bacteria (Wang et al., 2017). Therefore, all those factors led to high AAd concentrations in porewater of surface sediments.

Slezak et al. (1994) discovered that bacterial activity was retarded at AA concentrations > 10 μmol L^{-1} in long-term incubations of seawater cultures (24 to 110 h). Therefore, AAd in porewater might reduce bacterial metabolism and thus impact the microbial community in sediments, which is very important for studying marine sediment ecosystem. In addition, we speculated that high concentrations of AAd in sediments might be transported into the bottom seawater as Nedwell et al. (1994) found that DMS was emitted to water columns from the sediments. Up to date, there are only very limited studies on AAd in sediment, we cannot go further to address potential factors influencing AAd concentrations in porewater. For better understanding the source and fate of AAd in marine sediments, a detailed investigation of multiple parameters such as dissolved organic carbon, DMS, and DMSP in sediments is needed.

4.3 Degradation of DMSPd and AAd in the BS and YS

The microbial degradation rates of AAd in the BS and YS during summer were extremely higher than the total biological uptake of AAd (0.07-1.8 nmol L^{-1} d^{-1}) in the northern Gulf of Mexico in September 2011 (Tyssebotn et al., 2017), which might be due to the differences in the initial concentrations. Specifically, our study added exogenous AAd at the beginning of incubation. Nevertheless, we both found the microbial degradation rates at inshore stations were higher than those at offshore stations. In addition, almost all the production/degradation rates during summer and winter were independent with Chl *a*, which were also consistent with the results of Motard-Côté et al. (2016) and Tyssebotn et al. (2017).

The production/degradation rates of DMSPd, DMS, and AAd presented similar distributions in different sea areas during different seasons. For instance, DMS production rates were lower than AAd production rates at all stations in both summer and winter, which implied that AAd is produced by DMSP through more complicated demethylation processes besides enzymatic cleavage, which is thought to be the sole pathway of DMS production from DMSP. Meanwhile, low enzymatic cleavage ratio (<50%) during both summer and winter indicated that the enzymatic cleavage is not a dominant pathway of DMSP degradation (Ledyard and Dacey, 1996; Kiene and Linn, 2000b). Note that AAd productions rates were a little higher than the DMSPd degradation rates at some stations during both summer and winter, which might be owing to the direct production from DMSPp at those stations besides the exogenous DMSPd during the incubation experiments. In addition, AAd microbial degradation rates were always higher than the photochemical degradation rates, which suggested

that microbial degradation is a more important pathway of AAd removal relative to photochemical degradation.

Nevertheless, the production/degradation rates of DMSPd, DMS, and AAd showed seasonal and spatial variations as well. Higher production/degradation rates of DMSPd, DMS, and AAd in summer than in winter indicated that temperature promoted the degradation/production rates. In addition, the seasonal differences of bacteria abundance and light intensity also made great contributions to the different rates of microbial degradation and photochemical degradation, respectively. According to Liang et al. (2019), the abundances of *Vibrio* (γ-proteobacteria) averaged 1.4×10^6 copies L^{-1} in summer, which is significantly higher than in winter (Mann-Whitney test, $p < 0.01$), with a mean value of 1.9×10^5 copies L^{-1}. Significant seasonal differences in total bacterial abundance were also observed (Mann-Whitney test, $p < 0.001$). Meanwhile, the average light intensity in summer was 49400 lx, which was also higher than that in winter (34050 lx). All those factors led to high degradation/production rates in summer. In addition, Liang et al. (2019) also found that the dominant bacteria groups displayed different changing patterns in their abundance with seasons and sea areas. Specifically, the abundance of *V. campbellii* was higher in the YS than in the BS in summer ($p < 0.05$), whereas the abundance of *V. caribbeanicus* drastically decreased from the BS to the YS ($p < 0.05$). Therefore, the different microbial degradation/production rates of DMSPd, DMS, and AAd in different sea areas might result from the differences in bacteria species and abundance in the BS and YS. Moreover, the capabilities of diverse bacteria species to degrade AAd were different, which resulted in the inconsistence of AAd microbial degradation rates and rate constants in the comparison between inshore and offshore stations.

In order to estimate the contribution of different sources and sinks of AAd in surface seawater of the BS and YS, we applied the following equation:

$$dc/dt = r_{prod} - r_{bio} - r_{photo} + r_{other}$$

We assume AAd concentrations were at a steady state, so dc/dt = 0. AAd production rate (r_{prod}) was calculated from the AAd production rate constant times the in situ concentration. The AAd microbial degradation rate (r_{bio}) and photochemical degradation rate (r_{photo}) followed the same calculation method as r_{prod}. r_{other} represented other sources and sinks of AAd except production from DMSPd. According to these equations, the mean r_{prod}, r_{bio}, and r_{photo} in summer were 5.76 nmol L^{-1} h^{-1}, 8.43 nmol L^{-1} h^{-1}, and 2.83 nmol L^{-1} h^{-1}, respectively, thus there were certainly other sources of AAd at a rate of 5.50 nmol L^{-1} h^{-1}. These sources might be production from DMSPp, riverine inputs and other unknown sources. In winter, the mean r_{prod}, r_{bio}, and r_{photo} were 1.65 nmol L^{-1} h^{-1}, 2.66 nmol L^{-1} h^{-1}, and 1.32 nmol L^{-1} h^{-1}, respectively, thus the rate from other sources was 2.33 nmol L^{-1} h^{-1}, which was less than half of the rate in summer. This coincided with the AAd concentrations in surface seawater we observed in summer and winter.

5 Conclusions

We studied the horizontal and vertical distributions of AAd, DMS, and DMSP in the BS and YS during summer and winter. Significant seasonal variations were observed in the study area. AAd concentrations were relatively higher in the surface seawater during summer than during winter due to strong biological production from DMSP and abundant terrestrial inputs from rivers in summer. The distribution patterns of AAd during summer and winter were similar, that is, relatively high values of AAd emerged in the BS and the NYS and concentrations decreased from inshore to offshore areas in the SYS. In vertical profiles, high values of AAd, DMS, and DMSP were mostly observed in the upper layers with occasional high values in the bottom layers along three different transects. The average concentration sequence was AAd > DMSPt > DMS > DMSPd among all the three transects during summer, illustrating DMSPp as a DMS producer and terrestrial sources of AAd, whereas the sequence in winter along transects was AAd > DMSPt > DMSPd > DMS. DMS and AAd presented a stronger decrease from summer to winter than DMSP along transects. We also measured the

AAd concentrations in porewater of surface sediments. The extremely high values of AAd concentrations in porewater can be attributed to the abundant bacteria and active bacteria DMSP lyases in sediments. Moreover, the DMS and AAd production from DMSPd degradation and AAd degradation rates were always higher during summer than during winter. The AAd microbial degradation rates and rate constants were higher than the photochemical degradation rates and rate constants during both summer and winter. The AAd production and degradation experiments also proved other sources of AAd besides the production from DMSPd.

Author contribution. Xi Wu participated those two cruises to collect and analyse samples. Xi Wu and Chun-Ying Liu designed the on-deck experiments and Xi Wu carried them out. Xi Wu prepared the manuscript with contributions from all co-authors.

Competing interests. The authors declare that they have no conflict of interest.

Acknowledgments

We thank the captain and crew of the R/V ‘‘Dong Fang Hong 2’’ for their help during the investigations. This work was financially supported by the National Key Research and Development Program of China (No. 2016YFA0601301), the National Natural Science Foundation of China (Nos. 41676065 and 41176062) and the Fundamental Research Funds for the Central Universities (No. 201762032).

References

Alcolombri, U., Ben-Dor, S., Feldmesser, E., Levin, Y., Tawfik, D. S., and Vardi, A.: Identification of the algal dimethyl sulfide–releasing enzyme: A missing link in the marine sulfur cycle, Science, 348, 1466-1469, 2015.

Andreae, M. O., and Barnard, W. R.: Determination of trace quantities of dimethyl sulfide in aqueous solutions, Analytical Chemistry, 55, 608-612, 1983.

Andreae, M. O.: Dimethylsulfide in the water column and the sediment porewaters of the Peru upwelling area, Limnology and Oceanography, 30, 1208-1218, 1985.

Asher, E. C., Dacey, J. W. H., Stukel, M., Long, M. C., and Tortell, P. D.: Processes driving seasonal variability in DMS, DMSP, and DMSO concentrations and turnover in coastal Antarctic waters, Limnology and Oceanography, 62, 104-124, 2017.

Bajt, O., Šket, B., and Faganeli, J.: The aqueous photochemical transformation of acrylic acid, Marine chemistry, 58, 255-259, 1997.

Bentley, R., and Chasteen, T. G.: Environmental VOSCs—formation and degradation of dimethyl sulfide, methanethiol and related materials, Chemosphere, 55, 291-317, 2004.

Charlson, R. J., Lovelock, J. E., Andreae, M. O., and Warren, S. G.: Oceanic phytoplankton, atmospheric sulphur, cloud albedo and climate, Nature, 326, 655-661, 1987.

Curson, A. R. J., Liu, J., Bermejo Martínez, A., Green, R. T., Chan, Y., Carrión, O., Williams, B. T., Zhang, S.-H., Yang, G.-P., Bulman Page, P. C., Zhang, X.-H., and Todd, J. D.: Dimethylsulfoniopropionate biosynthesis in marine bacteria and identification of the key gene in this process, Nature Microbiology, 2, 17009, 2017.

Dacey, J. W., and Wakeham, S. G.: Oceanic dimethylsulfide: production during zooplankton grazing on phytoplankton, Science(Washington), 233, 1314-1316, 1986.

Dacey, J. W., and Blough, N. V.: Hydroxide decomposition of dimethylsulfoniopropionate to form dimethylsulfide, Geophysical Research Letters, 14, 1246-1249, 1987.

Deschaseaux, E. S., Jones, G. B., Deseo, M. A., Shepherd, K. M., Kiene, R. P., Swan, H. B., Harrison, P. L., and Eyre, B. D.: Effects of environmental factors on dimethylated sulfur compounds and their potential role in the antioxidant system of the coral holobiont, Limnology and Oceanography, 59, 758-768, 2014.

Espinosa, M. D. L. L., Martínez, A., Peralta, O., and Castro, T.: Spatial variability of dimethylsulfide (DMS) and dimethylsulfoniopropionate (DMSP) in the southern Gulf of Mexico, Environmental Chemistry, 13, 352-363, 2015.

Gibson, J. A. E., Swadling, K. M., and Burton, H. R.: Acrylate and Dimenthylsulfoniopropionate (DMSP) Concentrations during an Antarctic Phytoplankton Bloom, in: Biological and Environmental Chemistry of DMSP and Related Sulfonium Compounds, edited by: Kiene, R. P., Visscher, P. T., Keller, M. D., and Kirst, G. O., Springer US, Boston, MA, 213-222, 1996.

Jin, N.: Studies on Photochemical Process of Dimethylsulfide and its Transformation Rates in the Yellow Sea and the Bohai Sea, MS thesis, Ocean University of China, Qingdao, 2016.

Keller, M. D., Bellows, W. K., and Guillard, R. R. L.: Dimethyl sulfide production in marine phytoplankton, in: Biogenic Sulfur in the Environment, edited by: Saltzman, E. S., and Cooper, W. J., American Chemical Society, Washington, DC, 167-182, 1989.

Kiene, R. P., and Service, S. K.: Decomposition of dissolved DMSP and DMS in estuarine waters: dependence on temperature and substrate concentration, Marine Ecology Progress Series, 76, 1-11, 1991.

Kiene, R. P., and Service, S. K.: The Influence of Glycine Betaine on Dimethyl Sulfide and Dimethylsulfoniopropionate Concentrations in Seawater, in: Biogeochemistry of Global Change, edited by: Oremland, R. S., Springer US, Boston, M. A., 654-671, 1993.

Kiene, R. P., and Gerard, G.: Evaluation of glycine betaine as an inhibitor of dissolved dimethylsulfoniopropionate degradation in coastal waters, Marine Ecology Progress Series, 128, 121-131, 1995.

Kiene, R. P., Williams, L. P. H., and Walker, J. E.: Seawater microorganisms have a high affinity glycine betaine uptake system which also recognizes dimethylsulfoniopropionate, Aquatic microbial ecology, 15, 39-51, 1998.

Kiene, R. P., and Linn, L. J.: Distribution and turnover of dissolved DMSP and its relationship with bacterial production and dimethylsulfide in the Gulf of Mexico, Limnology and Oceanography, 45, 849-861, 2000a.

Kiene, R. P., and Linn, L. J.: The fate of dissolved dimethylsulfoniopropionate (DMSP) in seawater: tracer studies using ^{35}S-DMSP, Geochimica et Cosmochimica Acta, 64, 2797-2810, 2000b.

Kiene, R. P., and Slezak, D.: Low dissolved DMSP concentrations in seawater revealed by small-volume gravity filtration and dialysis sampling, Limnology and Oceanography: Methods, 4, 80-95, 2006.

Kinsey, J. D., Kieber, D. J., and Neale, P. J.: Effects of iron limitation and UV radiation on Phaeocystis antarctica growth and dimethylsulfoniopropionate, dimethylsulfoxide and acrylate concentrations, Environmental Chemistry, 13, 195-211, 2016.

Kirst, G. O., Thiel, C., Wolff, H., Nothnagel, J., Wanzek, M., and Ulmke, R.: Dimethylsulfoniopropionate (DMSP) in icealgae and its possible biological role, Marine Chemistry, 35, 381-388, 1991.

Lana, A., Bell, T., Simó, R., Vallina, S., Ballabrera-Poy, J., Kettle, A., Dachs, J., Bopp, L., Saltzman, E., and Stefels, J.: An updated climatology of surface dimethlysulfide concentrations and emission fluxes in the global ocean, Global Biogeochemical Cycles, 25, 3-25, 2011.

Ledyard, K. M., and Dacey, J. W.: Microbial cycling of DMSP and DMS in coastalandoligotrophicseawater, Limnology and Oceanography, 41, 33-40, 1996.

Lee, H. J., Jung, K. T., Foreman, M., and Chung, J. Y.: A three-dimensional mixed finite-difference Galerkin function

model for the oceanic circulation in the Yellow Sea and the East China Sea, Continental Shelf Research, 20, 863-895, 2000.

Levine, N. M., Varaljay, V. A., Toole, D. A., Dacey, J. W., Doney, S. C., and Moran, M. A.: Environmental, biochemical and genetic drivers of DMSP degradation and DMS production in the Sargasso Sea, Environmental microbiology, 14, 1210-1223, 2012.

Li, C.-Y., Zhang, D., Chen, X.-L., Wang, P., Shi, W.-L., Li, P.-Y., Zhang, X.-Y., Qin, Q.-L., Todd, J. D., and Zhang, Y.-Z.: Mechanistic Insights into Dimethylsulfoniopropionate Lyase DddY, a New Member of the Cupin Superfamily, Journal of molecular biology, 429, 3850-3862, 2017.

Li, C. X., Yang, G. P., Wang, B. D., and Xu, Z. J.: Vernal distribution and turnover of dimethylsulfide (DMS) in the surface water of the Yellow Sea, Journal of Geophysical Research: Oceans, 121, 7495-7516, 2016.

Liang, J., Liu, J., Wang, X., Lin, H., Liu, J., Zhou, S., Sun, H., and Zhang, X.-H.: Spatiotemporal dynamics of free-living and particle-associated Vibrio communities in the northern Chinese marginal seas, Applied and environmental microbiology, 85, e00217-00219, 2019.

Liu, C. Y., Wang, L. L., Yang, G. P., Chen, Y., and Li, P. F.: Determination of acrylic acid in seawater by high performance liquid chromatography and its application, Acta Oceanologica Sinica, 35, 172-176, 2013.

Liu, Q.: Analysis and Identification of Organic Compounds and Sifting of Items of Toxic Organic Compounds for the Water of Yalu River, Urban Environment & Urban Ecology, 14, 41-43, 2001.

Liu, S., Lou, S., Kuang, C., Huang, W., Chen, W., Zhang, J., and Zhong, G.: Water quality assessment by pollution-index method in the coastal waters of Hebei Province in western Bohai Sea, China, Marine pollution bulletin, 62, 2220-2229, 2011.

Liu, X., Huang, B., Huang, Q., Wang, L., Ni, X., Tang, Q., Sun, S., Wei, H., Liu, S., and Li, C.: Seasonal phytoplankton response to physical processes in the southern Yellow Sea, Journal of Sea Research, 95, 45-55, 2015.

Liu, Y., Liu, C.-Y., Yang, G.-P., Zhang, H.-H., and Zhang, S.-H.: Biogeochemistry of dimethylsulfoniopropionate, dimethylsulfide and acrylic acid in the Yellow Sea and the Bohai Sea during autumn, Environmental Chemistry, 13, 127-139, 2016.

Lovelock, J. E., Maggs, R. J., and Rasmussen, R. A.: Atmospheric dimethyl sulphide and the natural sulphur cycle, Nature, 237, 452–453, 1972.

Luan, Q., Sun, J., Shen, Z., Song, S., and Wang, M.: Phytoplankton assemblage of Yangtze River Estuary and the adjacent East China Sea in summer, 2004, Journal of Ocean University of China, 5, 123-131, 2006.

Malin, G., Turner, S. M., and Liss, P. S.: Sulfur: the plankton/climate connection, Journal of Phycology, 28, 590-597, 1992.

Malin, G., and Erst, G. O.: Algal Production of Dimethyl Sulfide and Its Atmospheric Role1, Journal of Phycology, 33, 889-896, 1997.

McParland, E. L., and Levine, N. M.: The role of differential DMSP production and community composition in predicting variability of global surface DMSP concentrations, Limnology and Oceanography, 64, 757-773, 2019.

Motard-Côté, J., Kieber, D. J., Rellinger, A., and Kiene, R. P.: Influence of the Mississippi River plume and non-bioavailable DMSP on dissolved DMSP turnover in the northern Gulf of Mexico, Environmental Chemistry, 13, 280-292, 2016.

Nedwell, D. B., Shabbeer, M. T., and Harrison, R. M.: Dimethyl sulphide in North Sea waters and sediments, Estuarine, Coastal and Shelf Science, 39, 209-217, 1994.

Nguyen, B. C., Mihalopoulos, N., Putaud, J. P., Gaudry, A., Gallet, L., Keene, W. C., and Galloway, J. N.: Covariations in oceanic dimethyl sulfide, its oxidation products and rain acidity at Amsterdam Island in the southern Indian Ocean,

Journal of Atmospheric Chemistry, 15, 39-53, 1992.

Ning, X., Lin, C., Su, J., Liu, C., Hao, Q., Le, F., and Tang, Q.: Long-term environmental changes and the responses of the ecosystems in the Bohai Sea during 1960–1996, Deep Sea Research Part II: Topical Studies in Oceanography, 57, 1079-1091, 2010.

Noordkamp, D. J. B., Gieskes, W. W. C., Gottschal, J. C., Forney, L. J., and Van Rijssel, M.: Acrylate in Phaeocystis colonies does not affect the surrounding bacteria, Journal of Sea Research, 43, 287-296, 2000.

Parsons, T. R., Maita, Y., and Lalli, C. M.: A manual of biological and chemical methods for seawater analysis, Pergamon Press, Oxford, 1984.

Quinn, P. K., and Bates, T. S.: The case against climate regulation via oceanic phytoplankton sulphur emissions, Nature, 480, 51-56, 2011.

Reisch, C. R., Moran, M. A., and Whitman, W. B.: Bacterial catabolism of dimethylsulfoniopropionate (DMSP), Frontiers in microbiology, 2, 1-12, 2011.

Seeberg-Elverfeldt, J., Schlüter, M., Feseker, T., and Kölling, M.: Rhizon sampling of porewaters near the sediment-water interface of aquatic systems, Limnology and oceanography: Methods, 3, 361-371, 2005.

Shenoy, D. M., and Patil, J. S.: Temporal variations in dimethylsulphoniopropionate and dimethyl sulphide in the Zuari estuary, Goa (India), Marine environmental research, 56, 387-402, 2003.

Shooter, D., and Brimblecombe, P.: Dimethylsulphide oxidation in the ocean, Deep Sea Research Part A. Oceanographic Research Papers, 36, 577-585, 1989.

Sicre, M. A., Peulve, S., Saliot, A., De Leeuw, J. W., and Baas, M.: Molecular characterization of the organic fraction of suspended matter in the surface waters and bottom nepheloid layer of the Rhone delta using analytical pyrolysis, Organic Geochemistry, 21, 11-26, 1994.

Sieburth, J. M.: Acrylic acid, an" antibiotic" principle in Phaeocystis blooms in Antarctic waters, Science, 132, 676-677, 1960.

Simó, R., Pedrós-Alió, C., Malin, G., and Grimalt, J. O.: Biological turnover of DMS, DMSP and DMSO in contrasting open-sea waters, Marine Ecology Progress Series, 203, 1-11, 2000.

Slezak, D., Puskaric, S., and Herndl, G. J.: Potential role of acrylic acid in bacterioplankton communities in the sea, Marine Ecology-Progress Series, 105, 191-191, 1994.

Spiese, C. E., Le, T., Zimmer, R. L., and Kieber, D. J.: Dimethylsulfide membrane permeability, cellular concentrations and implications for physiological functions in marine algae, Journal of Plankton Research, 38, 41-54, 2016.

Stefels, J.: Physiological aspects of the production and conversion of DMSP in marine algae and higher plants, Journal of Sea Research, 43, 183-197, 2000.

Steinke, M., Malin, G., Archer, S. D., Burkill, P. H., and Liss, P. S.: DMS production in a coccolithophorid bloom: evidence for the importance of dinoflagellate DMSP lyases, Aquatic Microbial Ecology, 26, 259-270, 2002.

Su, J.: Circulation dynamics of the China Seas north of 18°N, in: The Sea, edited by: Robinson, A. R., and Brink, K. H., Wiley, Hoboken, New Jersey, 483-505, 1998.

Sun, J., Liu, D., and Qian, S.: Preliminary study on seasonal succession and development pathway of phytoplankton community in the Bohai Sea, Acta Oceanologica Sinica, 20, 251-260, 2001.

Sun, J.: Distribution of Dimethyl Sulfur Compounds in China Marginal Seas and the Response of Their Algal Release to Acidificaiton MS thesis, Ocean University of China, Qingdao, 2017.

Sunda, W. G., Kieber, D. J., Kiene, R. P., and Huntsman, S.: An antioxidant function for DMSP and DMS in marine algae, Nature, 418, 317-320, 2002.

Tan, T.-T., Wu, X., Liu, C.-Y., and Yang, G.-P.: Distributions of dimethylsulfide and its related compounds in the Yangtze

(Changjiang) River Estuary and its adjacent waters in early summer, Continental Shelf Research, 146, 89-101, 2017.

Taylor, B. F., and Visscher, P. T.: Metabolic Pathways Involved in DMSP Degradation, in: Biological and Environmental Chemistry of DMSP and Related Sulfonium Compounds, edited by: Kiene, R. P., Visscher, P. T., Keller, M. D., and Kirst, G. O., Springer US, Boston, MA, 265-276, 1996.

Tyssebotn, I. M. B., Kinsey, J. D., Kieber, D. J., Kiene, R. P., Rellinger, A. N., and Motard-Côté, J.: Concentrations, biological uptake, and respiration of dissolved acrylate and dimethylsulfoxide in the northern Gulf of Mexico, Limnology and Oceanography, 62, 1198-1218, 2017.

Vairavamurthy, A., Andreae, M. O., and Brooks, J. M.: Determination of acrylic acid in aqueous samples by electron capture gas chromatography after extraction with tri-n-octylphosphine oxide and derivatization with pentafluorobenzyl bromide, Analytical Chemistry, 58, 2684-2687, 1986.

Wang, K.: Chracteristics of bacterial community in the sediments of the Bohai Sea and Yellow Seas, revealed by 454-Pyrosequencing, MS thsis, Ocean University of China, Qingdao, 2015.

Wang, P., Cao, H. Y., Chen, X. L., Li, C. Y., Li, P. Y., Zhang, X. Y., Qin, Q. L., Todd, J. D., and Zhang, Y. Z.: Mechanistic insight into acrylate metabolism and detoxification in marine dimethylsulfoniopropionate-catabolizing bacteria, Molecular Microbiology, 105, 674-688, 2017.

Wang, X., Cui, Z., Guo, Q., Han, X., and Wang, J.: Distribution of nutrients and eutrophication assessment in the Bohai Sea of China, Chinese Journal of Oceanology and Limnology, 27, 177-183, 2009.

Wei, H., Sun, J., Moll, A., and Zhao, L.: Phytoplankton dynamics in the Bohai Sea—observations and modelling, Journal of Marine Systems, 44, 233-251, 2004.

Wei, Q.-S., Liu, L., Zhan, R., Wei, X.-H., and Zang, J.-Y.: Distribution features of the chemical parameters in the Southern Yellow Sea in summer, Periodical of Ocean University of China, 40, 82-88, 2010.

Wolfe, G. V., Steinke, M., and Kirst, G. O.: Grazing-activated chemical defence in a unicellular marine alga, Nature, 387, 894-897, 1997.

Wu, X., Liu, C. Y., and Li, P. F.: Photochemical transformation of acrylic acid in seawater, Marine Chemistry, 170, 29-36, 2015.

Wu, X., Li, P. F., Liu, C. Y., Zhang, H. H., Yang, G. P., Zhang, S. H., and Zhu, M. X.: Biogeochemistry of Dimethylsulfide, Dimethylsulfoniopropionate, and Acrylic Acid in the Changjiang Estuary and the East China Sea, Journal of Geophysical Research: Oceans, 122, 10245-10261, 2017.

Yang, G. P., Song, Y. Z., Zhang, H. H., Li, C. X., and Wu, G. W.: Seasonal variation and biogeochemical cycling of dimethylsulfide (DMS) and dimethylsulfoniopropionate (DMSP) in the Yellow Sea and Bohai Sea, Journal of Geophysical Research: Oceans, 119, 8897-8915, 2014.

Yang, G. P., Zhang, S. H., Zhang, H. H., Yang, J., and Liu, C. Y.: Distribution of biogenic sulfur in the Bohai Sea and northern Yellow Sea and its contribution to atmospheric sulfate aerosol in the late fall, Marine Chemistry, 169, 23-32, 2015a.

Yang, J., Yang, G., Zhang, H., and Zhang, S.: Spatial distribution of dimethylsulfide and dimethylsulfoniopropionate in the Yellow Sea and Bohai Sea during summer, Chinese Journal of Oceanology and Limnology, 33, 1020-1038, 2015b.

Zhang, D.: The Study of Phytoplankton and Biosilicon in the Yellow Sea and the Bohai Sea, MS thesis, Tianjin University of Science and Technology, Tianjin, 2018.

Zindler, C., Peeken, I., Marandino, C. A., and Bange, H. W.: Environmental control on the variability of DMS and DMSP in the Mauritanian upwelling region, Biogeosciences, 9, 1041-1051, 2012.

Figure Captions

Figure 1: Locations of the sampling stations in the BS and YS during summer (a) and winter (b). (c) Schematic circulations and water masses in the BS and YS (Su, 1998; Lee et al., 2000). BSCC: Bohai Sea Coastal Current; YSCC: Yellow Sea Coastal Current; KCC: Korea Coastal Current; YSWC: Yellow Sea Warm Current; CRDW: Changjiang River Diluted Water; YSCWM: Yellow Sea Cold Water Mass.

Fig. 2. Horizontal distributions of Chl *a* (μg L^{-1}) and AAd (nmol L^{-1}) in the surface water of the BS and YS during summer and winter. a: Chl *a* in summer; b: AAd in summer; c: Chl *a* in winter; d: AAd in winter.

Fig. 3. Horizontal distributions of DMS (nmol L^{-1}), DMSPd (nmol L^{-1}), and DMSPp (nmol L^{-1}) in the surface water of the BS and YS during summer and winter. Data in summer and winter presented here were described by Jin (2016) and Sun (2017) respectively.

Fig. 4. Vertical profiles of temperature (°C), Chl *a* (μg L^{-1}), AAd (nmol L^{-1}), DMS (nmol L^{-1}), DMSPd (nmol L^{-1}), and DMSPt (nmol L^{-1}) along transect B57-63, transect B12-17, and transect H19-26 during summer. Kriging method is used for interpolating contours. The black dots represent sampling points.

Fig. 5. Vertical profiles of temperature (°C), Chl *a* (μg L^{-1}), AAd (nmol L^{-1}), DMS (nmol L^{-1}), DMSPd (nmol L^{-1}), and DMSPt (nmol L^{-1}) along transect B12-16 and transect H19-26 during winter. Kriging method is used for interpolating contours. The black dots represent sampling points.

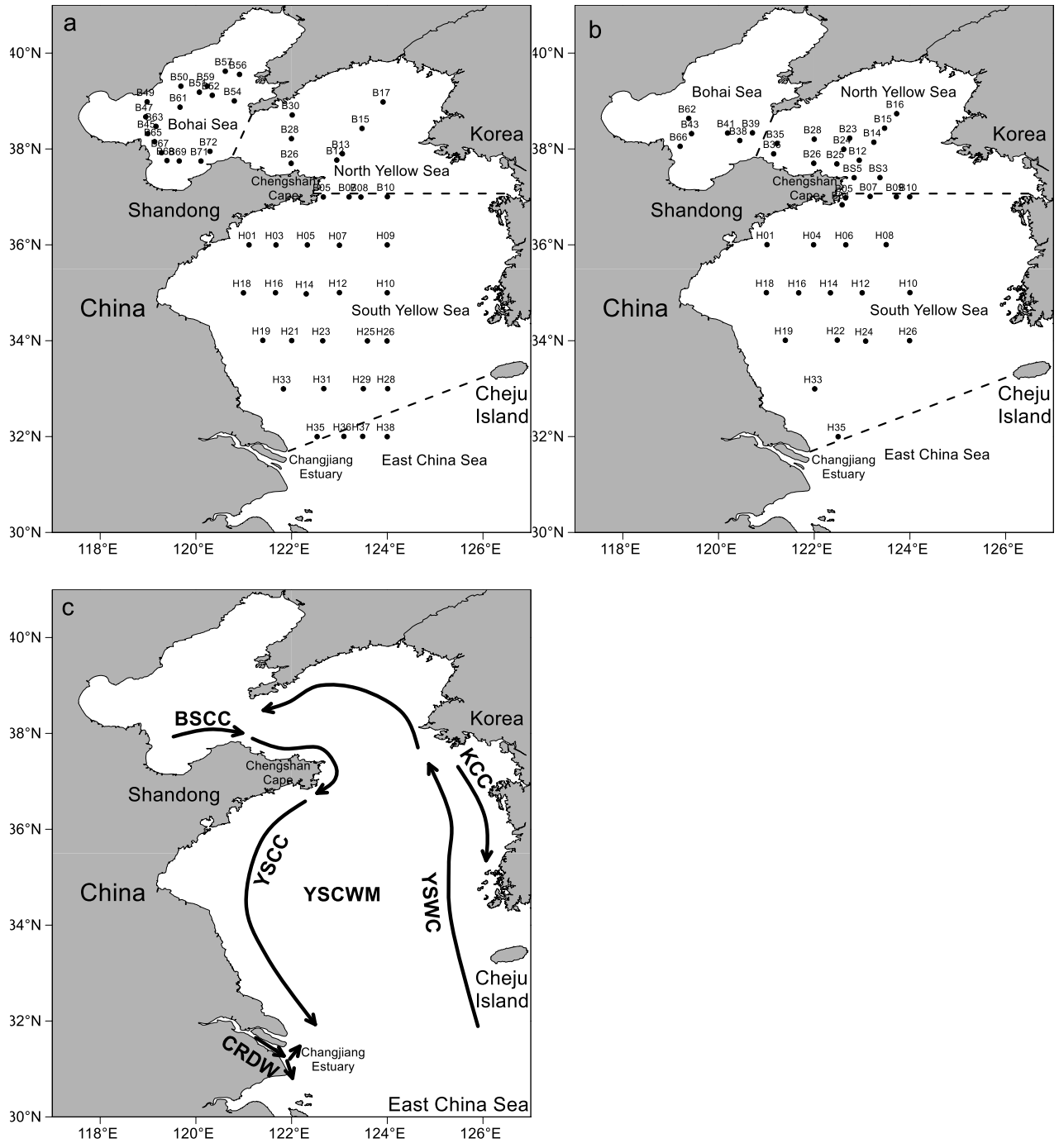

665

Fig. 1. Locations of the sampling stations in the BS and YS during summer (a) and winter (b). (c) Schematic circulations and water masses in the BS and YS (Su, 1998; Lee et al., 2000). BSCC: Bohai Sea Coastal Current; YSCC: Yellow Sea Coastal Current; KCC: Korea Coastal Current; YSWC: Yellow Sea Warm Current; CRDW: Changjiang River Diluted Water; YSCWM: Yellow Sea Cold Water Mass.

670

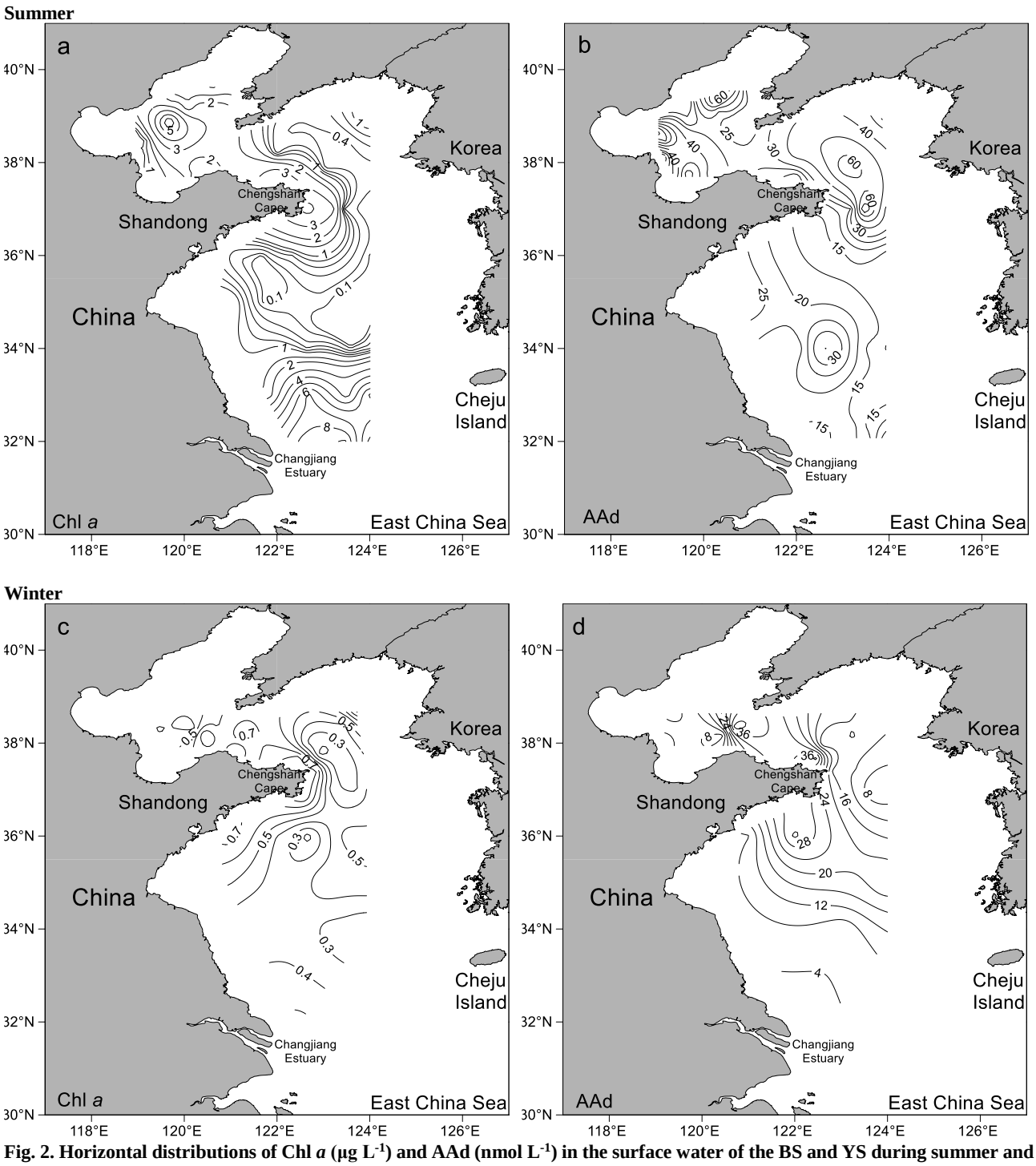

Fig. 2. Horizontal distributions of Chl *a* (μg L^{-1}) and AAd (nmol L^{-1}) in the surface water of the BS and YS during summer and winter. a: Chl *a* in summer; b: AAd in summer; c: Chl *a* in winter; d: AAd in winter.

Summer

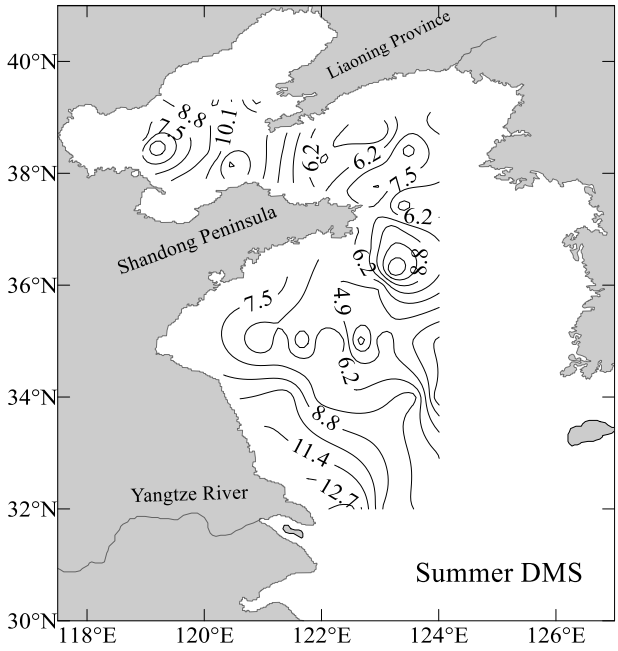
Liaoning Province
Shandong Peninsula
Yangtze River
Summer DMS
40°N
38°N
36°N
34°N
32°N
30°N
118°E
120°E
122°E
124°E
126°E

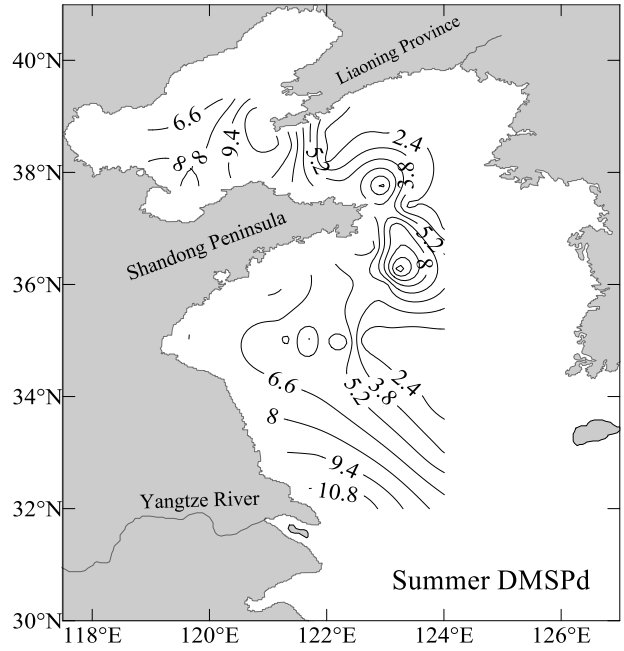
Liaoning Province
Shandong Peninsula
Yangtze River
Summer DMSPd
40°N
38°N
36°N
34°N
32°N
30°N
118°E
120°E
122°E
124°E
126°E

680

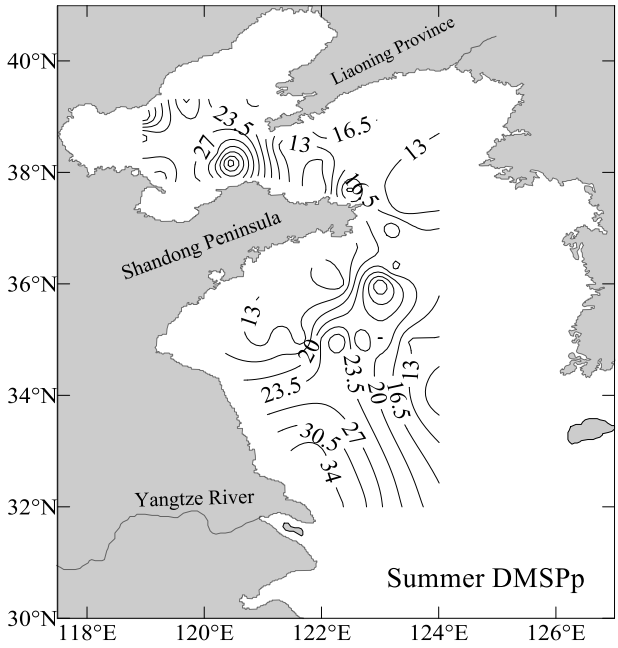
Liaoning Province
Shandong Peninsula
Yangtze River
Summer DMSPp
40°N
38°N
36°N
34°N
32°N
30°N
118°E
120°E
122°E
124°E
126°E

Winter

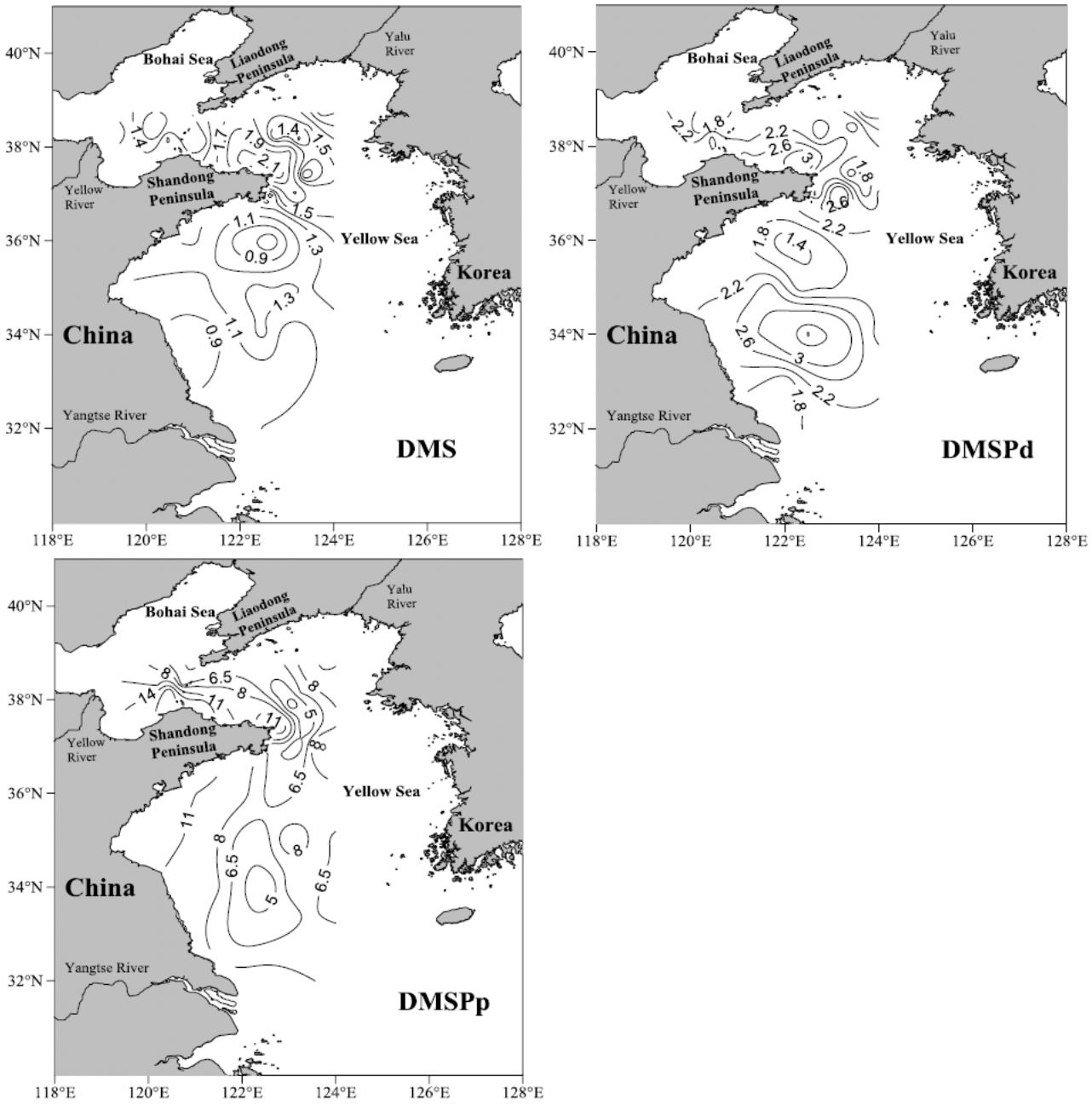

685 **Fig. 3. Horizontal distributions of DMS (nmol L^{-1}), DMSPd (nmol L^{-1}), and DMSPp (nmol L^{-1}) in the surface water of the BS and YS during summer and winter. Data in summer and winter presented here were described by Jin (2016) and Sun (2017) respectively.**

690

Transect B57-63

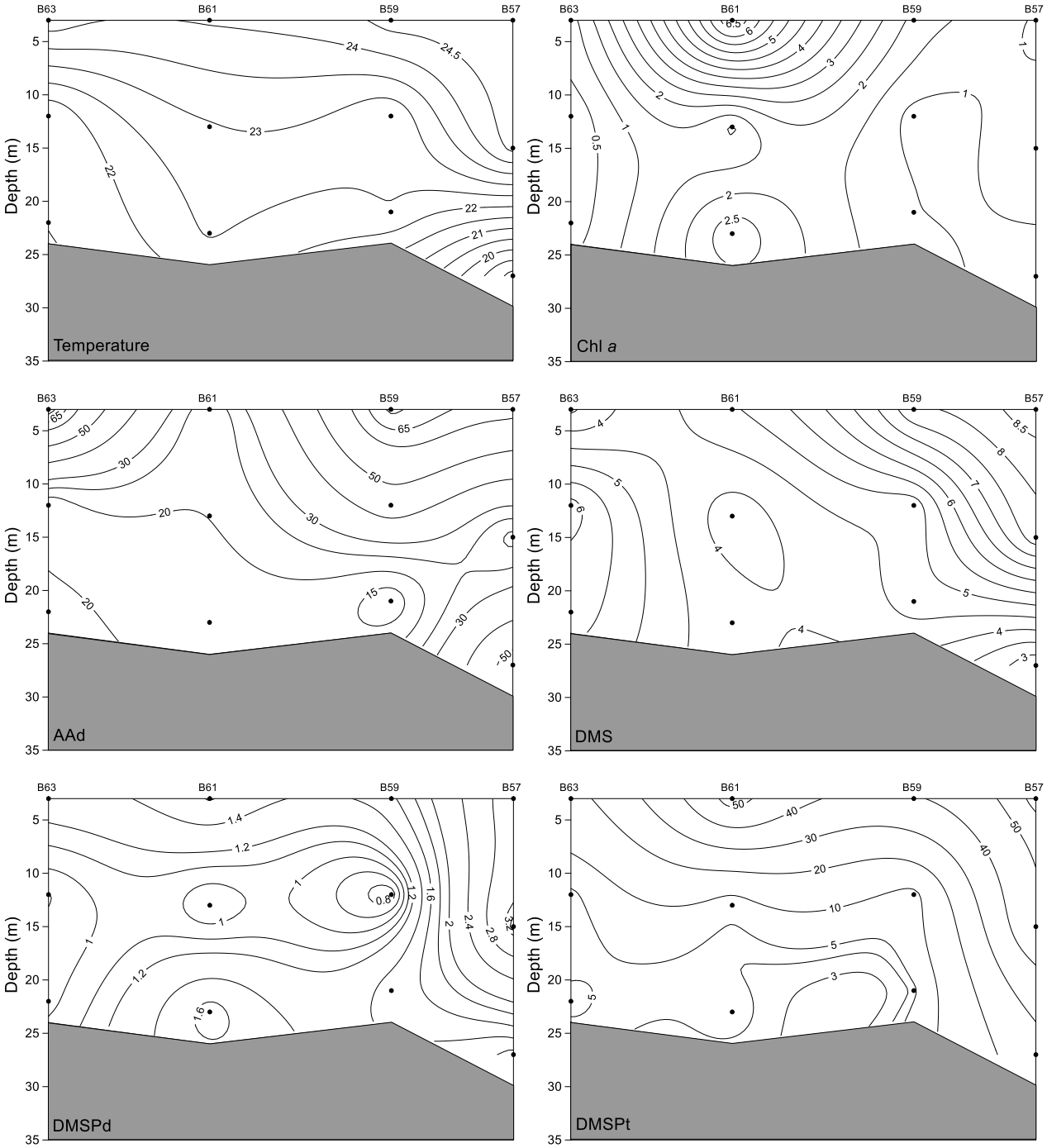

695

Transect B12-17

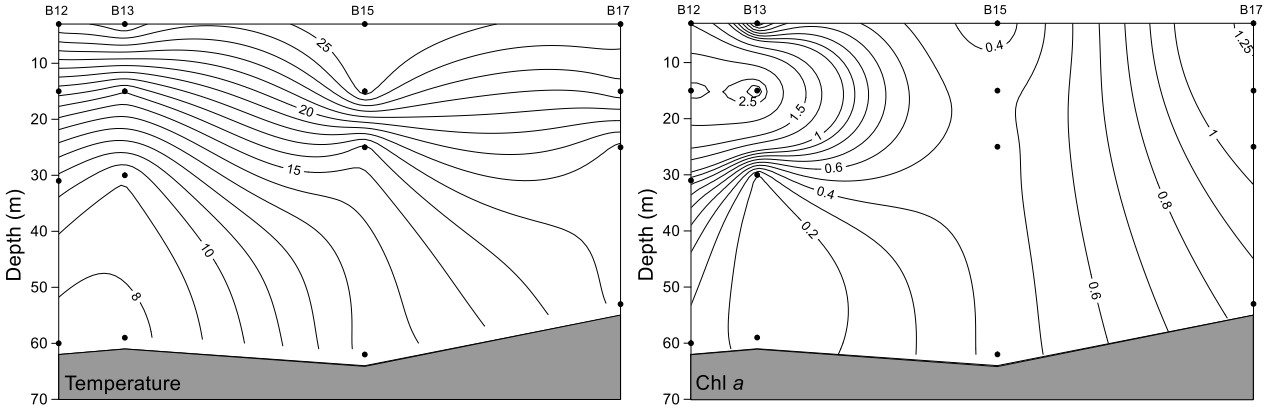

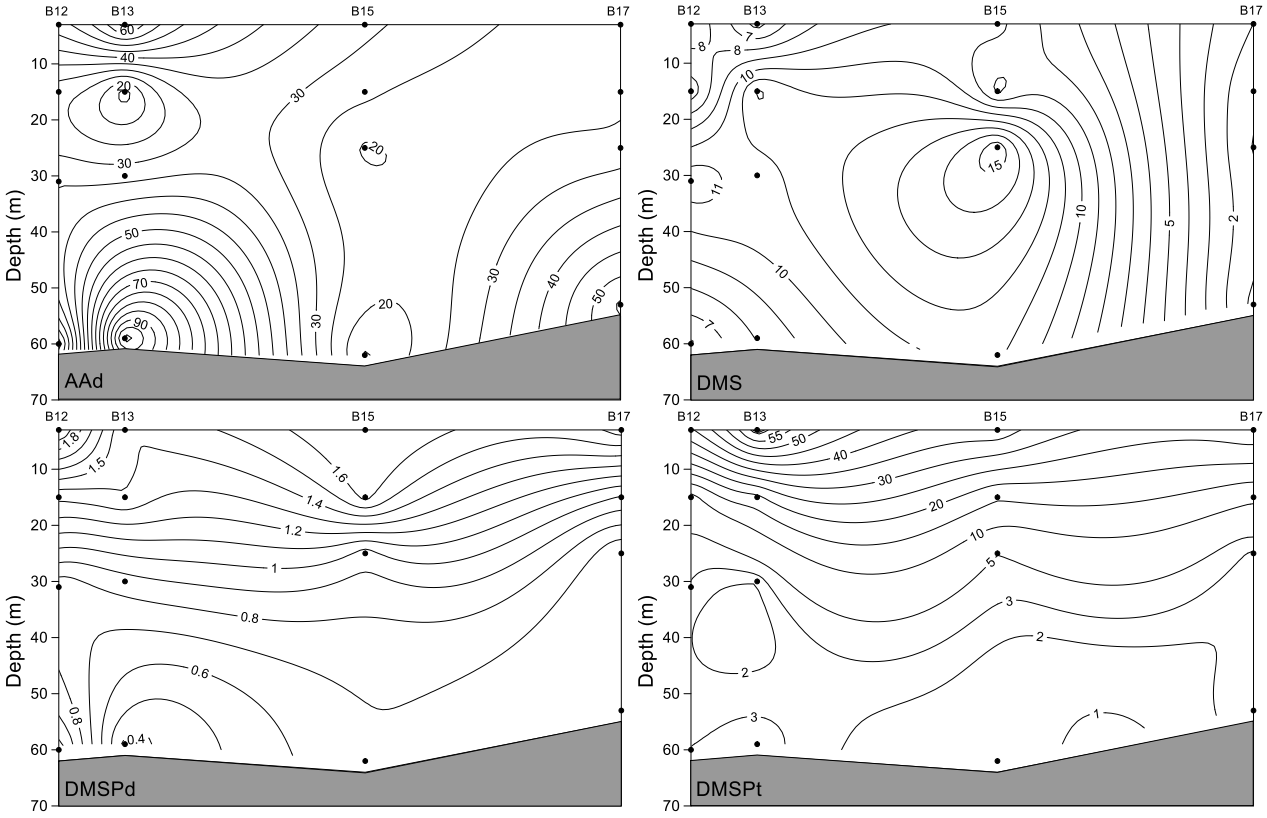

700

Transect H19-26

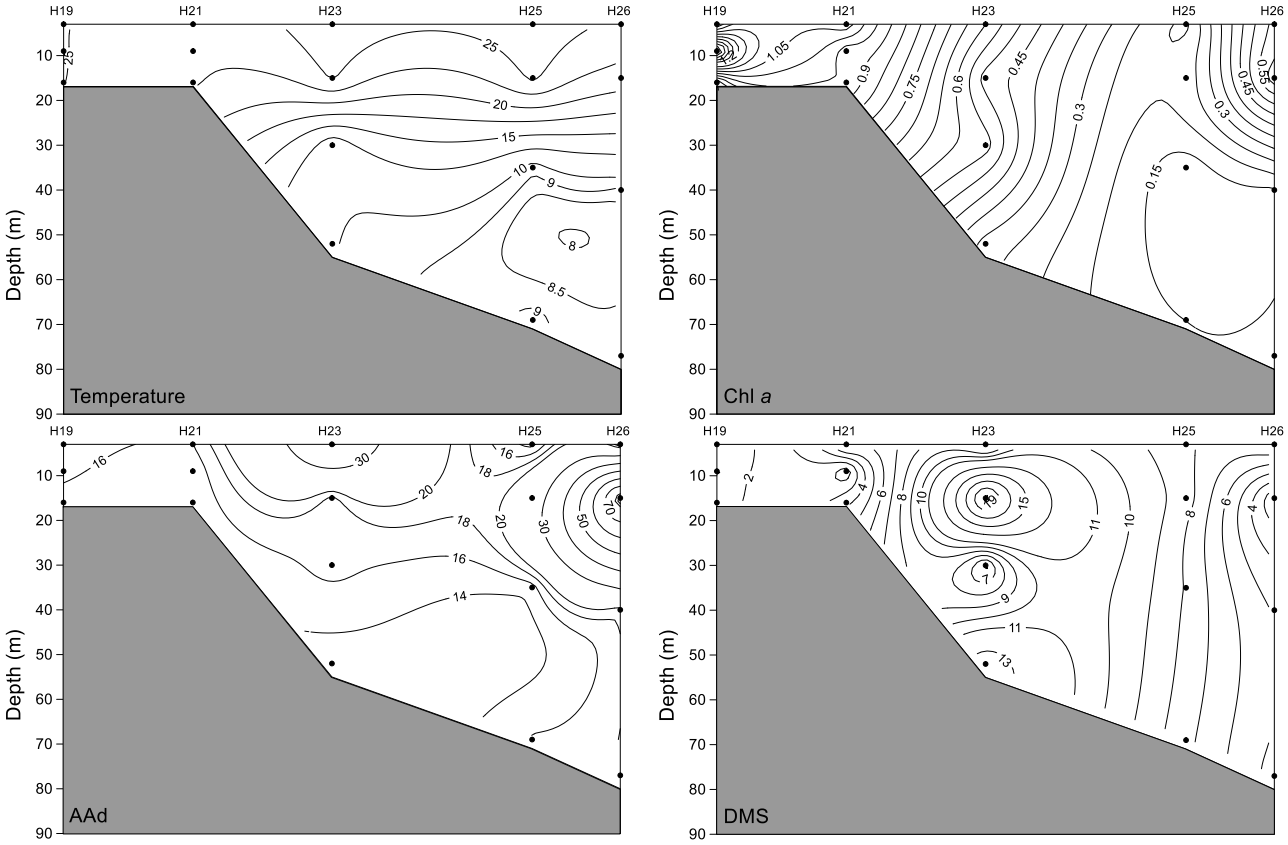

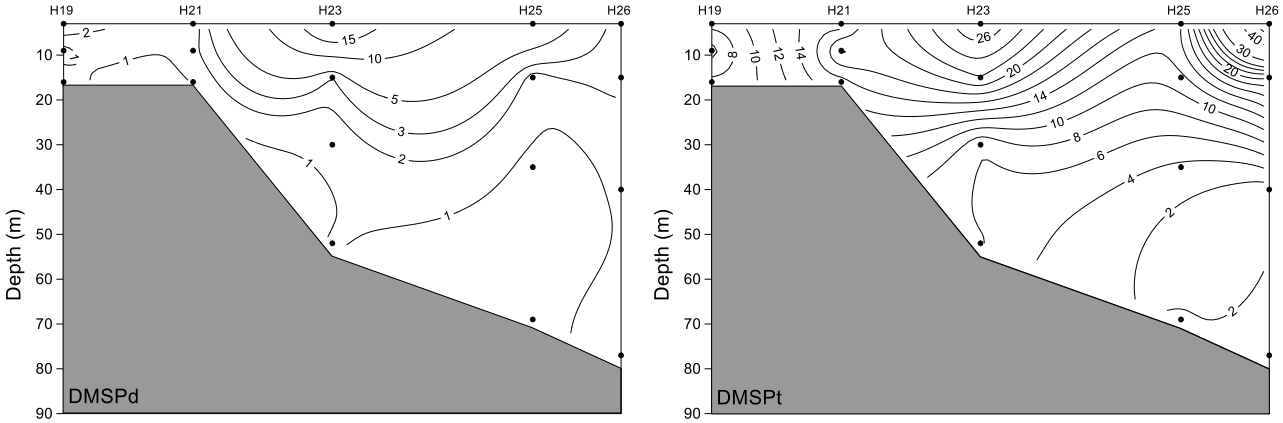

Fig. 4. Vertical profiles of temperature (°C), Chl *a* (µg L^{-1}), AAd (nmol L^{-1}), DMS (nmol L^{-1}), DMSPd (nmol L^{-1}), and DMSPt (nmol L^{-1}) along transect B57-63, transect B12-17, and transect H19-26 during summer. Kriging method is used for interpolating contours. The black dots represent sampling points.

Transect B12-16

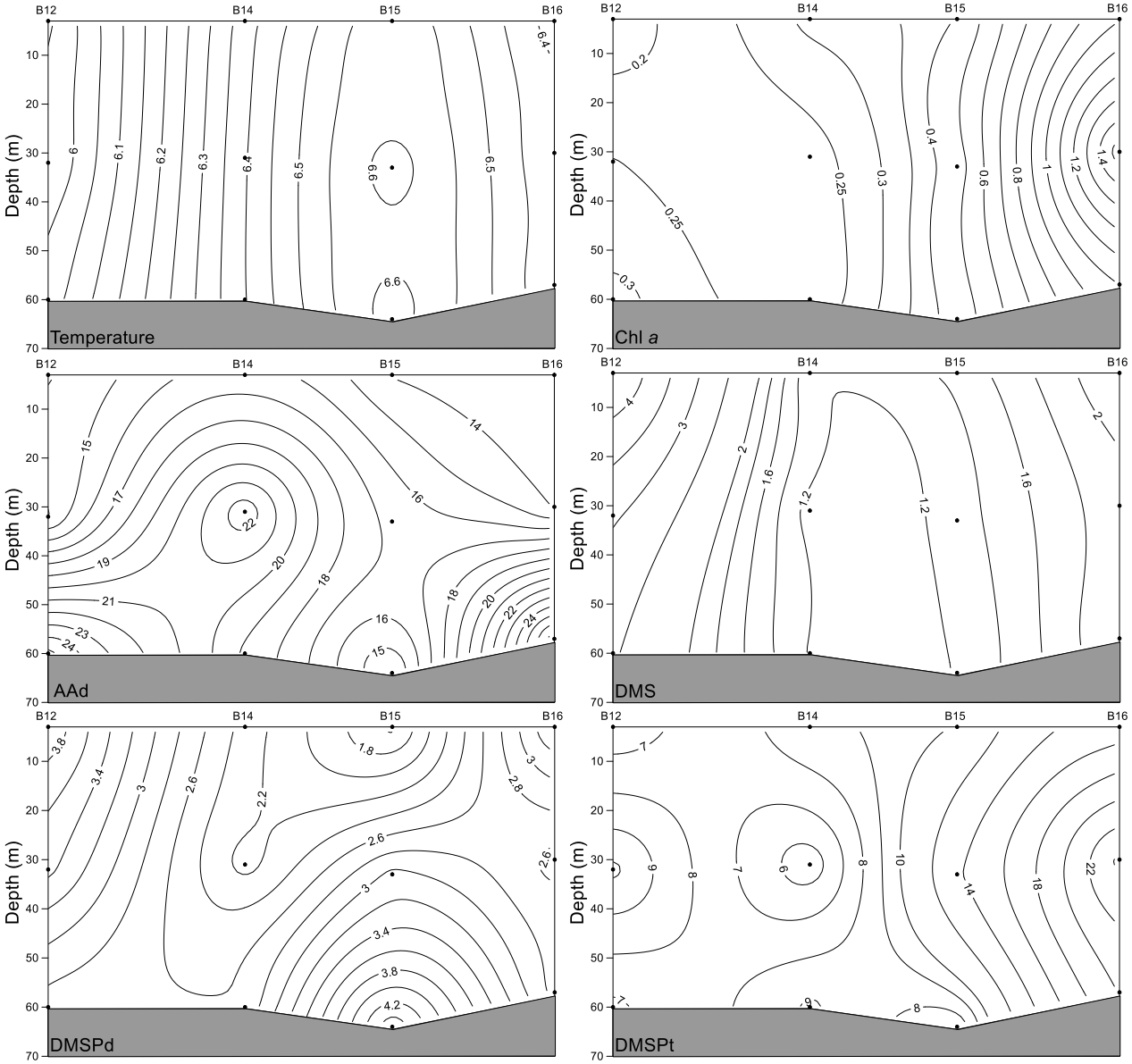

Transect H19-26

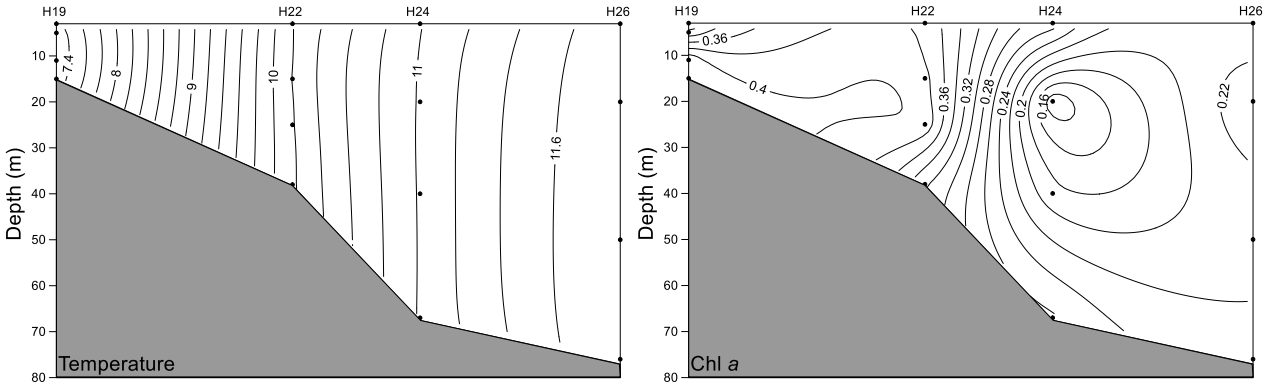

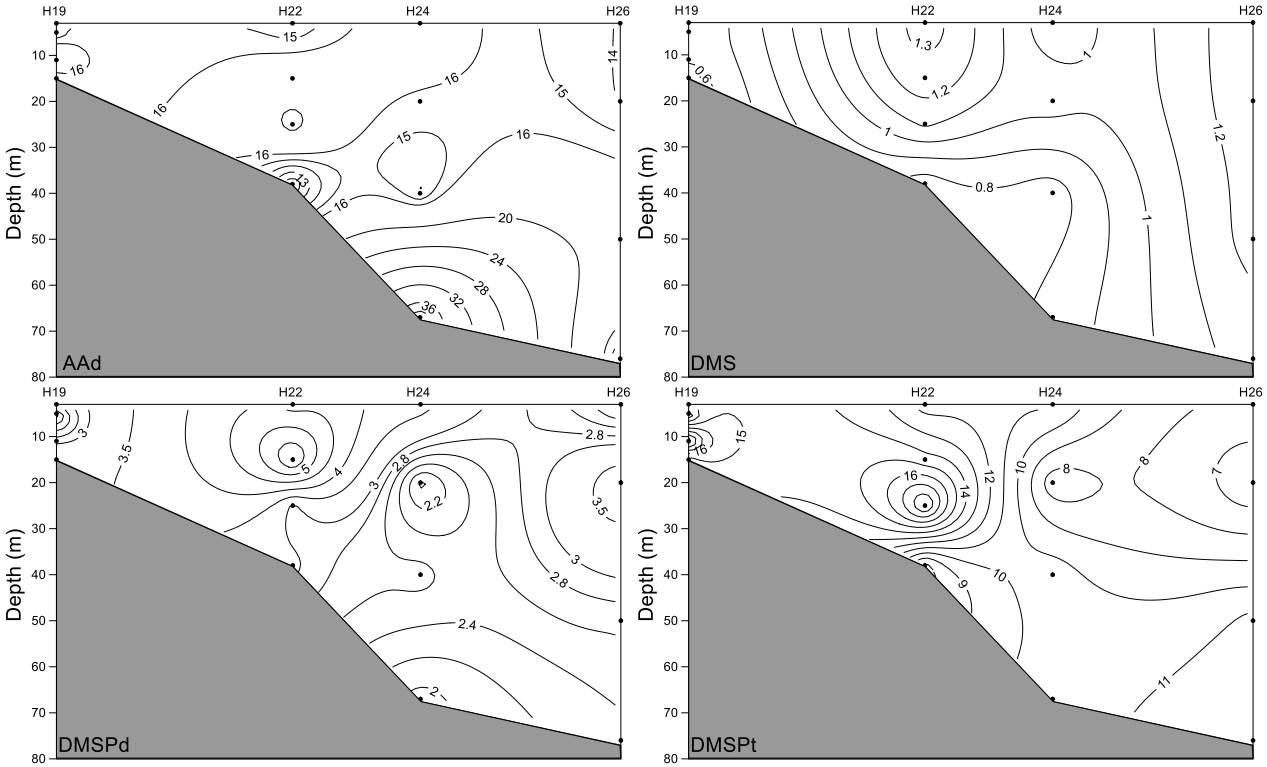

Fig. 5. Vertical profiles of temperature (°C), Chl *a* (µg L^{-1}), AAd (nmol L^{-1}), DMS (nmol L^{-1}), DMSPd (nmol L^{-1}), and DMSPt (nmol L^{-1}) along transect B12-16 and transect H19-26 during winter. Kriging method is used for interpolating contours. The black dots represent sampling points.

Table Captions

Table 1 Summary of the mean values (ranges) and the significance of seasonal differences of AAd, DMS, DMSPd, and DMSPt at surface seawater of the BS and YS and whole vertical profiles of transects during summer and winter. The significance of seasonal differences was obtained using Mann-Whitney test.

Table 2 Correlations between AAd, DMS, DMSP, and other biogeochemical parameters in the BS and YS during summer and winter. Pearson correlation test was used here.

Table 3 The AAd concentrations in porewater of surface sediments and in bottom seawater during summer 2015.

Table 4 Rates and rate constants of DMS and AAd production from DMSPd degradation and AAd degradation in the BS and YS during summer and winter.

735 **Table 1 Summary of the mean values (ranges) and the significance of seasonal differences of AAd, DMS, DMSPd, and DMSPt at surface seawater of the BS and YS and at whole vertical profiles of transects during summer and winter. The significance of seasonal differences was obtained using Mann-Whitney test.**

		AAd (nmol L^{-1})	DMS (nmol L^{-1})	DMSPd (nmol L^{-1})	DMSPt (nmol L^{-1})
Summer	Surface	30.01 ± 21.12 (10.53-92.29)	6.12 ± 3.01 (1.10-14.32)*	6.03 ± 3.45 (1.05-13.23)*	28.86 ± 14.15 (8.70-63.03)*
	B57-63	36.36 ± 23.57 (11.08-73.06)	5.51 ± 2.01 (2.57-8.79)	1.56 ± 0.84 (0.72-3.37)	22.94 ± 21.28 (4.12-56.61)
	B12-17	34.60 ± 26.00 (12.77-102.98)	7.37 ± 4.50 (0.74-15.76)	1.12 ± 0.48 (0.36-2.01)	15.45 ± 17.98 (1.90-63.03)
	H19-26	22.24 ± 18.25 (13.19-85.86)	6.44 ± 5.14 (0.79-21.98)	3.05 ± 4.92 (0.61-21.59)	13.67 ± 12.90 (1.11-55.14)
Winter	Surface	14.98 ± 7.22 (4.28-42.05)	1.38 ± 0.41 (0.54-2.22)*	2.30 ± 0.80 (1.16-4.29)*	10.39 ± 4.14 (2.36-22.21)*
	B12-16	17.68 ± 5.21 (13.94-27.69)	1.99 ± 1.02 (1.12-4.56)	2.92 ± 0.82 (1.54-4.55)	11.44 ± 5.89 (5.33-24.50)
	H19-26	17.08 ± 6.72 (11.04-39.47)	0.96 ± 0.29 (0.52-1.35)	3.06 ± 1.07 (1.92-6.06)	11.88 ± 3.97 (6.12-19.92)
Seasonal difference	Surface	$p < 0.001$	$p < 0.001$	$p < 0.01$	$p < 0.001$
	B12-16	$p < 0.05$	$p < 0.05$	$p < 0.001$	
	H19-26		$p < 0.001$	$p < 0.01$	

* collected from published MS theses (Jin, 2016; Sun, 2017)

Table 2 Correlations between AAd, DMS, DMSP, and other biogeochemical parameters in the BS and YS during summer and winter. Pearson correlation test was used here.

			T	S	Chl *a*	DMS	DMSPd	DMSPt	AAd	PO_4^{3-}	SiO_3^{2-}	NO_3^-	NO_2^-	NH_4^+
Summer	NYS surface	AAd	0.676*											
	SYS surface	AAd					0.626*							
	H19-26	DMSPt	0.549*	-0.555*							-0.486*	-0.510*	-0.510*	
	B12-17	DMSPd	0.742***	-0.626**						-0.745**	-0.737**	-0.784***	-0.792***	
		DMSPt	0.746***	-0.707**			0.725**			-0.630**	-0.850***	-0.721**	-0.730**	
	B57-63	DMS									-0.619*			
		DMSPd	0.593*	-0.843***						-0.806**				
		DMSPt		-0.867***		0.577*	0.745**			-0.762**		-0.650*	-0.647*	
Winter	BS surface	AAd	0.972*											
	H19-26	DMS	0.765***	0.691**						0.772**	0.824**			
		DMSPt	-0.605*	-0.618*										
	B12-16	DMS	-0.859***	-0.807**						-0.670*				
		DMSPd								-0.748*				
		DMSPt			0.930***						-0.852**			

*Significant at $p < 0.05$.
**Significant at $p < 0.01$.
***Significant at $p < 0.001$.

Table 3 The AAd concentrations in porewater of surface sediments and in bottom seawater during summer 2015.

Station	H10	H12	H14	H16	H19	H23	H25	H26	B12	B13	B61	B63
Sampling time	08-19 06:59	08-19 15:28	08-19 21:48	08-20 03:11	08-20 14:35	08-21 00:21	08-21 08:03	08-21 11:24	08-28 17:20	08-28 19:58	09-02 14:42	09-02 19:54
Porewater AAd (μmol L^{-1})	34.54	13.52	99.89	38.36	128.61	136.42	99.45	122.68	41.31	46.50	15.63	102.40
Bottom AAd (nmol L^{-1})	14.34	13.41	12.32	17.54	15.59	13.25	16.23	19.01	16.74	102.98	18.95	23.68

Table 4 Rates and rate constants of DMS and AAd production from DMSPd degradation and AAd degradation in the BS and YS during summer and winter.

Summer

Stations	SYS		NYS		BS	
	H19	H26	B12	B17	B57	B63
DMSPd degradation rates (nmol L^{-1} h^{-1})	3.12 ± 0.69	3.72 ± 0.28	1.44 ± 0.39	1.83 ± 1.08	5.76 ± 0.47	4.20 ± 0.36
DMSPd turnover times (h)	6.25	5.10	19.31	14.29	4.91	5.88
DMS production rates (nmol L^{-1} h^{-1})	0.55 ± 0.32	0.29 ± 0.12	0.33 ± 0.05	0.69 ± 0.09	0.90 ± 0.46	2.71 ± 0.36
AAd production rates (nmol L^{-1} h^{-1})	1.15 ± 0.31	1.90 ± 0.61	2.53 ± 0.64	1.15 ± 0.69	2.63 ± 0.35	5.20 ± 0.40
AAd microbial degradation rates (nmol L^{-1} h^{-1})	25.36 ± 13.15	22.10 ± 0.89	15.07 ± 0.52	11.84 ± 0.45	16.17 ± 0.52	24.92 ± 3.18
AAd photochemical degradation rates (nmol L^{-1} h^{-1})	3.16 ± 0.36	3.45 ± 2.08	0.91 ± 0.16	4.02 ± 0.34	0.67 ± 0.09	2.36 ± 0.14
AAd microbial degradation rate constants (h^{-1})	0.07 ± 0.05	0.36 ± 0.25	0.07 ± 0.004	0.30 ± 0.02	0.50 ± 0.03	0.03 ± 0.005
AAd photochemical degradation rate constants (h^{-1})	0.01 ± 0.009	0.02 ± 0.03	0.03 ± 0.006	0.14 ± 0.01	0.04 ± 0.005	0.12 ± 0.007

Winter

Stations	SYS		NYS	
	H19	H26	B12	B16
DMSPd degradation rates (nmol L^{-1} h^{-1})	2.26 ± 0.75	1.14 ± 0.50	1.92 ± 0.87	0.63 ± 0.59
DMSPd turnover times (h)	16.53	39.68	31.55	46.73
DMS production rates (nmol L^{-1} h^{-1})	0.08 ± 0.03	0.10 ± 0.02	0.09 ± 0.01	0.07 ± 0.05
AAd production rates (nmol L^{-1} h^{-1})	1.48 ± 0.29	1.22 ± 0.28	0.30 ± 0.25	0.91 ± 0.02
AAd microbial degradation rates (nmol L^{-1} h^{-1})	9.41 ± 0.59	4.73 ± 0.53	8.54 ± 0.08	18.66 ± 0.81
AAd photochemical degradation rates (nmol L^{-1} h^{-1})	4.30 ± 0.14	2.31 ± 0.48	2.72 ± 0.21	0.97 ± 0.46
AAd microbial degradation rate constants (h^{-1})	0.06 ± 0.01	0.36 ± 0.07	0.18 ± 0.002	0.29 ± 0.02
AAd photochemical degradation rate constants (h^{-1})	0.13 ± 0.005	0.06 ± 0.02	0.13 ± 0.01	0.05 ± 0.02